Approximate SIR Analysis in General Heterogeneous Cellular Networks

Haichao Wei, Na Deng, Wuyang Zhou, *Member, IEEE*, and Martin Haenggi, *Fellow, IEEE*

***Abstract*—The current cellular networks have evolved to be more randomly, irregularly, and heterogeneously deployed to meet the exponential growth of mobile data traffic and the demand for seamless coverage, making the signal-to-interference ratio (SIR) distribution more challenging to analyze. Therefore, in this paper we propose two simple approximative approaches to the SIR distribution of general heterogeneous cellular networks (HCNs) based on the ASAPPP method which stands for "approximate SIR analysis based on the Poisson point process" and the MISR (mean interference-to-signal ratio)-based gain for each individual tier of the HCNs. Specifically, we first establish a per-tier ASAPPP approximation to general HCNs and then present an effective gain ASAPPP method as a further simplification when the path loss exponents are the same for all the tiers, that is, we give an explicit expression for the effective gain $G_{\rm eff}$ of general HCNs such that the SIR distribution is obtained by scaling the SIR threshold θ to $\theta/G_{\rm eff}$. The asymptotic behavior for the tail of the SIR distribution is also given. Furthermore, to highlight the simplicity and effectiveness of the approximative approaches, we derive the exact distribution of the SIR in the two-tier HCNs modeled by β-Ginibre and Poisson point processes and compare it with the approximate results. The results demonstrate that the proposed approaches give a simple yet excellent approximation for the SIR distribution.**

***Index Terms*—Heterogeneous cellular networks, stochastic geometry, Poisson point process, signal-to-interference ratio, coverage probability.**

I. Introduction

A. Motivation

Heterogeneous cellular networks (HCNs) are widely regarded as a solution to address the challenge of the explosive mobile data traffic growth and to provide universal seamless coverage through deploying macro-, pico-, and femto-base stations (BSs) [2]. As one of the most important and general metrics, it is important to analyze the signal-to-interference ratio (SIR) distribution in the interference-limited HCNs to further obtain performance metrics such as outage, capacity, and throughput. The current theoretic analysis of the SIR distribution mostly focuses on the model based on homogeneous independent Poisson point processes (PPPs), introduced in [3]. However, the locations of the BSs in real deployments are spatially correlated, i.e, they exhibit some degree of repulsion or attraction. As shown in [4, 5], non-Poisson point processes such as the perturbed lattice, the β-Ginibre point process, etc., can capture the spatial characteristics of the real deployments better than the PPP. For such non-Poisson networks, the analysis of the SIR is significantly more difficult than that of Poisson networks and can be obtained merely by large-scale complicated simulations or at best be expressed using combinations of infinite sums and integrals. Although one can investigate any desired scenario to any desired depth of detail through simulations, this would require the simulation of every possible scenario of interest separately, including all possible choices of the deployment parameters. Even worse, as the number of the combinations of different deployment parameters rises exponentially with the undergoing transformation from the single-tier macrocellular network to the multi-tier HCN, an exhaustive simulation study of every possible scenario of interest will be extremely time-consuming and expensive, if not completely unfeasible. As as result, with only a limited number of scenarios investigated, the insight obtained is restricted, making it difficult to draw inferences for other cases. Hence it is necessary to explore efficient techniques that provide good approximations of the SIR distribution for general HCN models.

B. Related Work

The homogeneous independent PPP (HIP[1]) model usually yields highly tractable results for HCNs [3, 6–8] but does not capture the spatial dependence between base stations (BSs). However, for non-Poisson deployments, exact results of the SIR distribution are hard to derive or, even though they could be derived, the resulting expressions are very complex to compute [9–11]. As a result, it is almost impossible to figure out how the network performance is affected by the parameters, such as the density, transmit power, etc. In [12], the authors provide the Padé approximation for the coverage probability of a cellular network model where the BSs form a β-Ginibre point process (β-GPP), but the results show that the Padé approximation becomes very inaccurate as the SIR threshold increases. In addition, since the Maclaurin coefficient computation in the approximation involves multiple-level and infinite

Haichao Wei and Wuyang Zhou are with Key Laboratory of Wireless-Optical Communications, Chinese Academy of Sciences, School of Information Science and Technology, University of Science and Technology of China (USTC), Hefei, Anhui Province, 230026, P. R. China (e-mail: weihc@mail.ustc.edu.cn, wyzhou@ustc.edu.cn). Na Deng is with the Shanghai Institute, Huawei Technology Co., Ltd, Pudong New Area, Shanghai 201206, P. R. China (e-mail: dengna1@huawei.com). Martin Haenggi is with the Dept. of Electrical Engineering, University of Notre Dame, Notre Dame 46556, USA (e-mail: mhaenggi@nd.edu).

Part of this paper was presented at GLOBECOM'15 [1].

This work was supported by National programs for High Technology Research and Development (2014AA01A707) and by the US NSF grants CCF 1216407 and CCF 1525904.

[1] A model whose tiers are independent Poisson point processes is called HIP model. Its SIR distribution is equivalent to that of the single-tier PPP model when the power path loss law with Rayleigh fading and strongest-BS association are adopted [6].

integrals, sums and products, the numerical computation of the coverage probability is still complex and time-consuming. Moreover, the Padé approximation can be expected to be even more complex when applied in the heterogeneous scenarios.

Fortunately, as shown in [6, 13–15], the coverage probability $P_{\mathrm{c}}(\theta) \triangleq P(\mathrm{SIR} > \theta)$ for general single-tier networks can be tightly approximated by merely scaling the threshold θ to θ/G, i.e., $P_{\mathrm{c}}(\theta) \approx P_{\mathrm{c}}^{\mathrm{PPP}}(\theta/G)$, where $P_{\mathrm{c}}^{\mathrm{PPP}}(\theta)$ is the coverage probability of Poisson networks and G can be quantified using the mean interference-to-signal ratio (MISR) and is thus called MISR-based gain. We show that the MISR-based method can be applied to general HCNs that are modeled by arbitrary (but stationary and independent) point processes.

C. Contributions

The main objective of this paper is to present two simple approximative approaches that yield highly tractable results for the SIR distribution in general HCNs. Both are extensions of the ASAPPP-based approximation [16], which stands for "approximate SIR analysis based on the PPP", to general HCNs using the MISR-based gain for each individual tier. In the first approach, we use the ASAPPP method to approximate the coverage probabilities of the typical user served by the BS in each tier and then sum the probabilities to obtain the complete coverage probability, thus we call it *per-tier ASAPPP* method. The per-tier ASAPPP method provides an asymptotic lower bound for the coverage probability. The second approach is applicable when the path loss exponents are the same for all tiers. It constitutes a further simplification of the per-tier ASAPPP method by giving an explicit expression of the effective gain of HCNs. The SIR distribution can then be directly obtained by scaling the SIR threshold with the effective gain, thus we call it *effective gain ASAPPP* method. Besides, we employ the ASAPPP method to approximately characterize the tail of the SIR distribution of general HCNs.

Moreover, to highlight the simplicity and effectiveness of the approximative approaches, we compare the exact distribution of the SIR in the two-tier HCNs modeled by β-Ginibre and Poisson point processes with the approximative approaches. Our results demonstrate that both methods are excellent approximations to the SIR distribution in general HCNs with simple expressions.

II. System Model

We consider a coverage-oriented heterogeneous cellular network (HCN) model comprising K types of nodes, i.e., a K-tier heterogeneous cellular network, consisting of independent and stationary point processes Φ_k, $k = 1, 2, \ldots, K$, which are the locations of the BSs in the k-th tier, and G_k is the corresponding MISR-based gain. Let μ_k, λ_k, and α_k be the transmit power, node density, and path loss exponent of the k-th tier, respectively. We assume that each user is associated with the BS that offers the strongest average received power. Due to the stationarity of all Φ_k, we consider the typical user located at the origin. We assume a power path loss law $\ell(x) = |x|^{-\alpha_k}$ associated with node x, where k is the tier x belongs to, and independent Rayleigh fading h_x with unit mean, $\mathbb{E}(h_x) = 1$. Thus, the received SIR of the typical user is expressed as

$$\mathrm{SIR} \triangleq \frac{S}{I} = \frac{\mu_{x_0}\ell(x_0)h_{x_0}}{\sum\limits_{x\in \bigcup\limits_{k\in[K]} \Phi_k\setminus\{x_0\}} \mu_x \ell(x) h_x}, \qquad (1)$$

where $[K] \triangleq \{1, 2, \ldots, K\}$, x_0 denotes the location of the serving BS of the typical user and μ_x denotes the transmit power of node x: if $x \in \Phi_k$, $\mu_x = \mu_k$. Then, the coverage probability is obtained as the total probability of the disjoint events that the typical user accesses a BS from tier k, given by

$$\begin{aligned} P_{\mathrm{c}}(\theta) &= \mathbb{P}(\mathrm{SIR} > \theta) \\ &= \sum_{k\in[K]} \mathbb{P}(\mathrm{SIR} > \theta, x_0 \in \Phi_k), \end{aligned} \qquad (2)$$

where θ is the SIR threshold.

We list the main symbols and parameters used in the paper in Table I.

III. The ASAPPP Approach

A. The ASAPPP Approach for Single-tier Networks

Under the SIR threshold model for reception, the coverage probability $P_{\mathrm{c}}(\theta)$ is equivalent to the complementary cumulative distribution (ccdf) $\bar{F}_{\mathrm{SIR}}(\theta)$ of the SIR, i.e., $P_{\mathrm{c}}(\theta) \equiv \bar{F}_{\mathrm{SIR}}(\theta)$. If the BSs form a homogeneous PPP or HIP model with Rayleigh fading, the coverage expression is tractable exactly [6]. For the second-simplest model (β-Ginibre point process) with Rayleigh fading, the coverage probability can be expressed using a combination of infinite sums and integrals [5]. In all other cases it may be impossible to find exact expressions. Hence there is a critical need for good approximation techniques. It has recently been shown in [6, 13–16] that the SIR ccdfs for single-tier networks modeled by different point processes are approximately just horizontally shifted versions of each other (in dB). Due to its tractability, the Poisson network provides a baseline to obtain the coverage probability curves of other models, and the horizontal gap (SIR gain) at the target probability p is defined as

$$G_{\mathrm{p}}(p) \triangleq \frac{\bar{F}_{\mathrm{SIR}}^{-1}(p)}{\bar{F}_{\mathrm{SIR}_{\mathrm{PPP}}}^{-1}(p)}, \qquad p \in (0, 1), \qquad (3)$$

where $\bar{F}_{\mathrm{SIR}}^{-1}$ is the inverse of the SIR ccdf. The gap is often defined as a function of θ, expressed as

$$G(\theta) \triangleq G_{\mathrm{p}}\big(P_{\mathrm{c}}^{\mathrm{PPP}}(\theta)\big) = \frac{\bar{F}_{\mathrm{SIR}}^{-1}(P_{\mathrm{c}}^{\mathrm{PPP}}(\theta))}{\theta}. \qquad (4)$$

The asymptotic gain G (whenever the limit exists) is defined as

$$G \triangleq \lim_{p\to 1} G_{\mathrm{p}}(p) = \lim_{\theta\to 0} G(\theta), \qquad (5)$$

which can be quantified using the mean interference-to-signal ratio (MISR) and thus is called MISR-based gain. For a network with base stations located at Φ with serving BS x_0, the MISR at the typical user is defined as [6]

$$\mathrm{MISR} \triangleq \mathbb{E}\left\{\frac{I}{\mathbb{E}_h(S)}\right\} = \mathbb{E}\left\{\frac{\sum_{x\in\Phi\setminus\{x_0\}} \mu_x \ell(x)}{\mu_{x_0}\ell(x_0)}\right\}. \qquad (6)$$

TABLE I. SYMBOLS AND DESCRIPTION

Symbol	Description
Φ_k, λ_k, μ_k	The point process of the BSs in tier k and its density and transmit power
Φ_k^{PPP}	The Poisson point process approximate for Φ_k
$\ell(x)$, h_x	The path loss attenuation and Rayleigh fading from the BS located at x to the user located at the origin
α_k	The path loss exponent of tier k
MISR	The mean interference-to-signal ratio
EFIR	The expected fading-to-interference ratio
G_k, G_∞^k	The asymptotic gains at $\theta = 0$ (MISR-based gain) and at ∞ (EFIR-based gain) for tier k
$\hat{G}$, G_{eff}	The per-tier overall gain and effective gain for HCNs with the SIR threshold at 0
$\hat{G}_\infty$, G_∞^{eff}	The per-tier overall gain and effective gain for HCNs with the SIR threshold at ∞
$\mathrm{NP}(\Phi)$	The nearest point in Φ to the origin
$\bar{F}_{\mathrm{SIR}}(\theta)$	The complementary cumulative distribution of SIR
β	The parameter for β-Ginibre point process to adjust the regularity

$\mathbb{E}_h(S) = \mu_{x_0}\ell(x_0)$ is the signal power averaged over the fading. Hence the MISR is independent of the fading model. The MISR for Poisson networks is $\mathrm{MISR}_{\mathrm{PPP}} = 2/(\alpha-2)$, which also holds for the HIP model with an arbitrary number of tiers, densities and transmit powers [6]. In general, the SIR distribution satisfies $F_{\mathrm{SIR}}(\theta) \sim \mathrm{MISR}\ \theta$ as $\theta \to 0$ in the Rayleigh fading scenario[2]. Therefore, using (6), the asymptotic gain G defined in (5) can be expressed as

$$G = \frac{\mathrm{MISR}_{\mathrm{PPP}}}{\mathrm{MISR}}. \tag{7}$$

As illustrated in [14, 15], the MISR-based gain provides a good approximation for the entire SIR distribution, i.e., we have $G(\theta) \approx G$. Consequently, the SIR distribution of non-Poisson networks can be accurately approximated by that of a Poisson network through scaling the threshold θ with the MISR-based gain G, i.e., $P_{\mathrm{c}}(\theta) \approx P_{\mathrm{c}}^{\mathrm{PPP}}(\theta/G)$, and the approximation is asymptotically exact as $\theta \to 0$. That is why this approach of approximating SIR distribution is called ASAPPP method [16], which stands for "approximate SIR analysis based on the PPP" and can also be read as "as a PPP", indicating that the network is first treated as if it forms a PPP and then a shift is applied to the SIR distribution.

B. The ASAPPP Approach for Heterogeneous Networks

Since the cellular networks are currently undergoing a major transformation to be heterogeneously deployed, the dynamic nature and complexity of heterogeneous networks due to different types and combinations of point processes, densities, and transmit powers, make it even harder to get analytical expressions of the SIR distribution except for the HIP model. Thus, we investigate how to extend the ASAPPP method to general HCNs using the MISR-based gains of the individual tiers constituting the HCNs. The coverage probability is expressed as the total probability of several disjoint events, i.e., the coverage event is partitioned according to the user being served by a certain tier. When a user accesses a BS from a non-Poisson tier, this tier is treated as a PPP with the corresponding threshold θ shifted to θ/G in the SIR distribution. Meanwhile, the interference from the other tiers is assumed to be approximated by that from another Poisson network, which is another instance of "as a PPP". Approximating a repulsive point process[3] with a PPP yields an interference power that stochastically dominates the actual interference power [17]. Consequently, the resulting coverage probability is a lower bound to the exact coverage probability, which turns out to be tight from our numerical results. Based on the above method, an overall effective SIR gain is further given to directly obtain the SIR distribution of HCNs by scaling the SIR threshold of Poisson networks.

The main difficulty in the generalization from single-tier to multi-tier networks is the interference characterization. In the single-tier case, having x_0 as the serving BS eliminates one interferer from the BS process Φ and also implies that the remaining interfering BSs are further away. In HCNs, the interference from *all* BS belonging to the non-serving tier needs to be considered, while still taking into account that none of them is stronger (on average) than the serving one. Moreover, the power levels in each tier and, more importantly, the path loss models in each tier may be different.

IV. K-TIER HETEROGENEOUS CELLULAR NETWORKS

A. Main Result

We first focus on general K-tier HCNs and then specialize to the case when the path loss exponents are the same. Let $\delta \triangleq 2/\alpha$ and $T(\alpha,\theta) \triangleq 1 + \theta^\delta \int_{\theta^{-\delta}}^{\infty} \frac{1}{1+t^{\alpha/2}} \mathrm{d}t$, which can be expressed in terms of the Gaussian hypergeometric function ${}_2F_1$ as [18]

$$T(\alpha,\theta) = {}_2F_1(1, -\delta, 1-\delta, -\theta), \tag{8}$$

and the coverage probability of the networks modeled by a homogeneous PPP is given as $P_{\mathrm{c}}^{\mathrm{PPP}}(\theta) = 1/T(\alpha,\theta)$ [19]. The same expression is valid for general HIP models [7]. The following theorem gives an accurate approximation and asymptotic bound on the coverage probability of general HCNs.

Theorem 1. *Let $\delta_i \triangleq 2/\alpha_i$ and*

$$\hat{P}_{\mathrm{c}}(\theta) \triangleq \sum_{k\in[K]} \int_0^\infty \exp\Bigg(- rT(\alpha_k, \theta/G_k) - \sum_{i\in[K]^!} \frac{\pi\lambda_i (\frac{\mu_i}{\mu_k})^{\delta_i}}{(\pi\lambda_k)^{\alpha_k/\alpha_i}} r^{\frac{\alpha_k}{\alpha_i}} T(\alpha_i,\theta)\Bigg) \mathrm{d}r. \tag{9}$$

[2]The MISR-based gain for general fading models is investigated in [6, 15].

[3]A point process whose pair correlation function is at most 1.

For K-tier HCNs where the typical user is served by the BS with the strongest average received power, the coverage probability $P_{\rm c}(\theta)$ is approximated by

$$P_{\rm c}(\theta) \approx \hat{P}_{\rm c}(\theta). \quad (10)$$

Moreover,

$$P_{\rm c}(\theta) \gtrsim \hat{P}_{\rm c}(\theta), \quad (11)$$

where '$\gtrsim$' stands for an asymptotic lower bound, i.e., $\exists t > 0$ s.t. $P_{\rm c}(\theta) > \hat{P}_{\rm c}(\theta)\ \forall \theta < t$.

Proof: We first define the nearest-point operator

$$\mathrm{NP}(\Phi) \triangleq \arg\min\{x \in \Phi \colon |x|\} \quad (12)$$

and the reduced point process

$$\Phi^! \triangleq \Phi \setminus \{\mathrm{NP}(\Phi)\}. \quad (13)$$

When a user is served by a BS in the k-th tier, we have $x_0 = \mathrm{NP}(\Phi_k)$. Letting $\ell_k(x) = \ell(x)$ if $x \in \Phi_k$, and $\mathcal{A}_{i,k} = \{\mu_i \ell_i(y) \leq \mu_k \ell_k(x_0)\}$, we have

$$\begin{aligned}
&\mathbb{P}(\mathrm{SIR} > \theta, x_0 \in \Phi_k)\\
&= \mathbb{E}\left\{\exp\left(-\theta \frac{\sum\limits_{x\in\Phi_k^!}\mu_k\ell_k(x)h_x + \sum\limits_{i\in[K]^!}\sum\limits_{y\in\Phi_i}\mu_i\ell_i(y)h_y}{\mu_k\ell_k(x_0)}\right)\mathbf{1}_{x_0\in\Phi_k}\right\}\\
&= \mathbb{E}\left\{\prod_{i\in[K]^!}\prod_{y\in\Phi_i}\left(1+\frac{\theta\mu_i\ell_i(y)}{\mu_k\ell_k(x_0)}\right)^{-1}\mathbf{1}_{\mathcal{A}_{i,k}}\prod_{x\in\Phi_k^!}\left(1+\frac{\theta\ell_k(x)}{\ell_k(x_0)}\right)^{-1}\right\}\\
&\overset{(a)}{\sim} \mathbb{E}\left\{\prod_{i\in[K]^!}\prod_{y\in\Phi_i}\left(1+\frac{\theta\mu_i\ell_i(y)}{\mu_k\ell_k(x_0)}\right)^{-1}\mathbf{1}_{\mathcal{A}_{i,k}}\prod_{x\in\Phi_k^{!\mathrm{PPP}}}\left(1+\frac{\theta\ell_k(x)}{G_k\ell_k(x_0)}\right)^{-1}\right\}\\
&\overset{(b)}{\gtrsim} \mathbb{E}\left\{\prod_{i\in[K]^!}\prod_{y\in\Phi_i^{\mathrm{PPP}}}\left(1+\frac{\theta\mu_i\ell_i(y)}{\mu_k\ell_k(x_0)}\right)^{-1}\mathbf{1}_{\mathcal{A}_{i,k}}\prod_{x\in\Phi_k^{!\mathrm{PPP}}}\left(1+\frac{\theta\ell_k(x)}{G_k\ell_k(x_0)}\right)^{-1}\right\}\\
&\overset{(c)}{=} \int_0^\infty f_k(r)\exp\Bigg(-2\pi\lambda_k\int_r^\infty \frac{t\mathrm{d}t}{1+\frac{G_k t^{\alpha_k}}{\theta r^{\alpha_k}}}\\
&\qquad - \sum_{i\in[K]^!}\pi\lambda_i\left(r^{\alpha_k\delta_i}\left(\frac{\mu_i}{\mu_k}\right)^{\delta_i} + \int_{r^{\frac{\alpha_k}{\alpha_i}}(\frac{\mu_i}{\mu_k})^{\frac{1}{\alpha_i}}}^\infty \frac{2t\mathrm{d}t}{1+\frac{\mu_k t^{\alpha_i}}{\theta\mu_i r^{\alpha_k}}}\right)\Bigg)\mathrm{d}r\\
&= \int_0^\infty 2\pi\lambda_k r\exp\Bigg(-\pi\lambda_k r^2 T(\alpha_k,\theta/G_k)\\
&\qquad - \sum_{i\in[K]^!}\pi\lambda_i r^{\alpha_k\delta_i}\left(\frac{\mu_i}{\mu_k}\right)^{\delta_i} T(\alpha_i,\theta)\Bigg)\mathrm{d}r\\
&= \int_0^\infty \exp\Big(-rT(\alpha_k,\theta/G_k) - \sum_{i\in[K]^!}\rho_{i,k}r^{\frac{\alpha_k}{\alpha_i}}T(\alpha_i,\theta)\Big)\mathrm{d}r, \quad (14)
\end{aligned}$$

where $\rho_{i,k} = \frac{\pi\lambda_i(\frac{\mu_i}{\mu_k})^{\delta_i}}{(\pi\lambda_k)^{\alpha_k/\alpha_i}}$, $[K]^! = [K]\setminus\{k\}$, and $f_k(r) = 2\lambda_k\pi r e^{-\lambda_k\pi r^2}$ is the distribution of $|\mathrm{NP}(\Phi_k^{\mathrm{PPP}})|$ [20]. Step (a) uses the asymptotically exact ASAPPP approximation of Φ_k by shifting θ to θ/G_k and replacing Φ_k by a PPP denoted by Φ_k^{PPP}. In step (b) the interference from Φ_i is upper bounded by that of a PPP denoted by Φ_i^{PPP} with the same density as Φ_i, which provides a lower bound for the coverage probability[4]. Since ASAPPP is asymptotically exact and accurate for a large range of θ, the approximation in step (a) is asymptotically exact and step (b) gives an asymptotic lower bound and provides an approximation for the coverage probability. The probability generating functional (PGFL) of the PPP [21] is used in step (c).

The final result follows by summing over $[K]$. ■

If the path loss exponents are all equal, we have the following simplification.

Corollary 1. *When $\alpha_1 = \alpha_2 = \ldots = \alpha_k = \alpha$,*

$$\hat{P}_{\rm c}(\theta) = \sum_{k\in[K]}\frac{1}{T(\alpha,\theta/G_k) + \sum\limits_{i\in[K]^!}\frac{\lambda_i}{\lambda_k}(\frac{\mu_i}{\mu_k})^{\delta}T(\alpha,\theta)}. \quad (15)$$

In this method, we calculate the probabilities of the disjoint events that the user is served by BSs from different tiers and then approximate each one using ASAPPP with the MISR-based gain of individual tier, thus we call it *per-tier ASAPPP method*. When the per-tier ASAPPP method is applied to K-tier HIP networks, (15) reduces to $\hat{P}_{\rm c}(\theta) = 1/T(\alpha,\theta)$, which is the exact result for K-tier HIP networks as mentioned above. When $\lambda_i\mu_i^{\delta}, i \in [K]$, are the same for all tiers, $\lim\limits_{K\to\infty}\hat{P}_{\rm c}(\theta) = 1/T(\alpha,\theta)$, no matter what the G_k are.

In the following, we take $K = 2$ as an example, i.e., we consider two-tier HCNs comprising the macro-BSs (MBSs) and the pico-BSs (PBSs) and then divide this class of models into two types, where for the first one, one tier is a non-Poisson network and the other is a Poisson network; while for the second one, both tiers are non-Poisson networks.

B. Non-Poisson/PPP Deployment

In this subsection, we consider two kinds of non-Poisson point processes, namely, the β-GPP and the lattice model.

1) Special Case: β-GPP/PPP: The locations of the MBSs Φ_1 are modeled by a β-GPP, and the locations of the PBSs Φ_2 are modeled by a PPP. Through simulations and visual inspection, we find that the MISR-based gain of the β-GPP is quite exactly $G \approx 1 + \beta/2$, irrespective of α, as can be seen in Figure 1. Therefore, the coverage probability of the user served by a β-GPP network is approximately the same as that of a user served by a Poisson network and scaling the SIR threshold θ to $\theta/(1+\beta/2)$, which is verified in Figure 2.

Figure 3 and 4 show the coverage probability of the heterogeneous networks with different α and β when $\lambda_1 = \lambda_2 = 10^{-5}$ and $\mu_1 = \mu_2 = 1$. It is apparent that the approximation is excellent over a wide range of θ, which validates the effectiveness of the proposed per-tier ASAPPP method. The tiny gap between each simulation and its corresponding approximation can be attributed to the approximation of the interference from the non-Poisson tier by that of a PPP, which yields the asymptotic lower bound.

[4]Clustered tiers can also be included with a change in the inequality in step (b). If the tiers constituting the HCNs are all clustered or Poisson, the inequality becomes '$\lesssim$', and if the HCNs are a combination of clustered and repulsive point processes, the inequality becomes '$\approx$'.

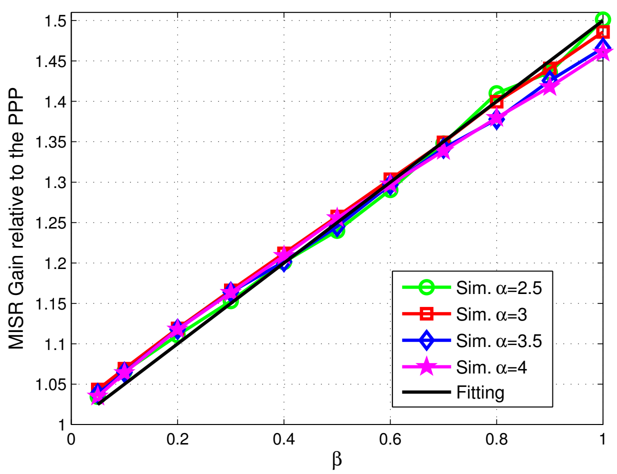

Fig. 1. The MISR-based gain of the β-GPP for different α.

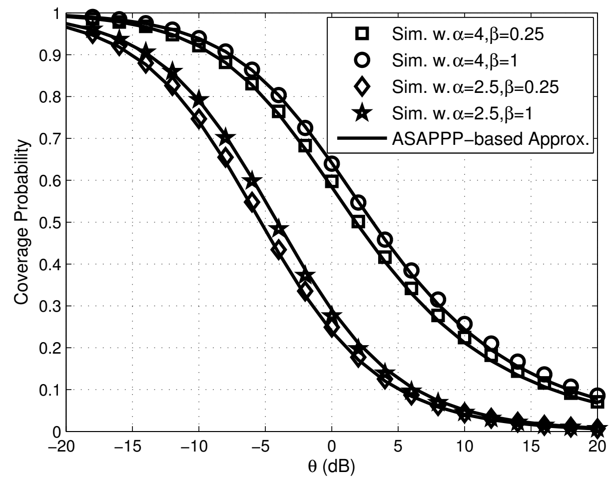

Fig. 2. The ASAPPP-based approximation of β-GPP networks for different α and β.

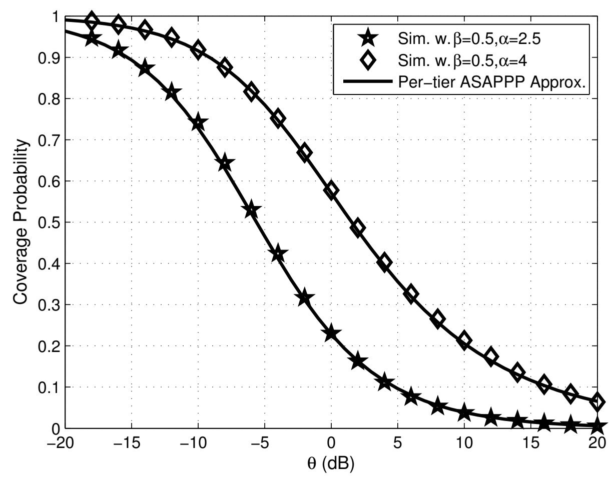

Fig. 3. The per-tier ASAPPP approximation of β-GPP/PPP networks for $\beta = 0.5$.

2) Special Case: Square lattice/PPP: The locations of the MBSs Φ_1 are modeled by a randomly translated square lattice, and the locations of the PBSs Φ_2 are modeled by a PPP. From [6], the MISR of the square lattice is quite exactly half of that of the PPP, irrespective of the path loss exponent, i.e., $G_{\text{square}} \approx 2$, and the ASAPPP approximation for the single-tier square lattice networks is tight for coverage probabilities over a wide range of θ. Figure 5 shows the coverage probability with different α when $\lambda_1 = \lambda_2 = 10^{-5}$ and $\mu_1 = \mu_2 = 1$, which further corroborates the effectiveness of the per-tier ASAPPP method. Comparing Figs. 4 and 5, we can see that the gap between the simulation and its corresponding approximation is bigger than in the β-GPP/PPP case. For instance, when $\theta = -10\,\text{dB}$, the relative errors in Fig. 4 between the approximate and the simulation results are 1.7%, 1.0%, 1.0%, and 1.5% for $\alpha = 4, 3.5, 3$ and 2.5, respectively while the ones in Fig. 5 are 2.6%, 1.6%, 1.6%, and 4.6%, respectively. It can be explained as follows: the square lattice is more regular than the GPP, thus the approximation of the interference from the square lattice tier by that of a PPP leads to a less accurate approximation.

C. Non-Poisson/Non-Poisson Deployment

In this subsection, we again consider two types of HCNs: one is composed of two β-GPPs, and the other consists of a lattice and a β-GPP.

1) Special Case: Two β-GPPs: The locations of the MBSs Φ_1 and the PBSs Φ_2 are two independent β-GPPs. Figure 6 shows the coverage probability with different α when $\lambda_1 = \lambda_2 = 10^{-5}$, $\mu_1 = \mu_2 = 1$ and $\beta = 1$, which again demonstrates the accuracy of the per-tier ASAPPP approximation. Letting $\omega \triangleq \frac{\lambda_2}{\lambda_1}\left(\frac{\mu_2}{\mu_1}\right)^{\delta}$, we also see from (15) that the coverage performance for the two-tier independent GPP networks is the worst with $\omega = 1$ (while better than that of Poisson networks) because in this case the independence between the two tiers reduces the regularity property of a single GPP the most. Conversely, as ω tends to zero or infinity, these HCNs tend to single-tier GPP networks, since one of the two tiers dominates.

2) Special Case: Square lattice/β-GPP: Here, the locations of the MBSs Φ_1 form a randomly translated square lattice, and the locations of the PBSs Φ_2 form a β-GPP. Figure 7 gives the coverage probability for different α when $\lambda_1 = \lambda_2 = 10^{-5}$, $\mu_1 = \mu_2 = 1$ and $\beta = 1$. We can see that similar to the case of square lattice/PPP, the ASAPPP-based approximations are tight when θ tends to zero and become slightly less accurate as θ increases. The reason is the same, i.e., the higher regularity of the square lattice deployment leads to the less accurate approximation in the HCNs.

D. Effective Gain of K-Tier HCNs

In the per-tier ASAPPP method, we add up the probabilities of the disjoint events that the user accesses the BSs from different tiers using the corresponding MISR-based gains. In the following, we give an overall (or effective) SIR gain of

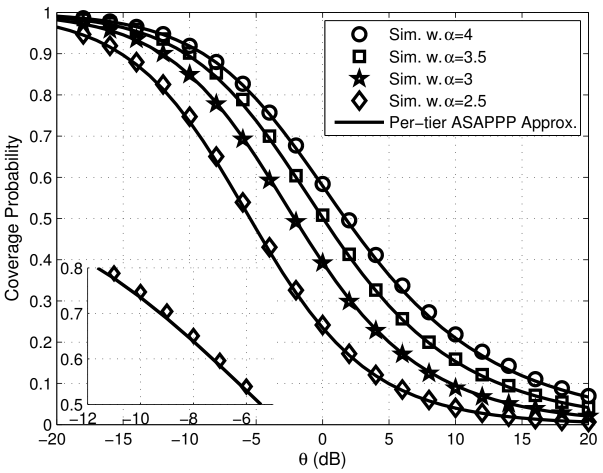

Fig. 4. The per-tier ASAPPP approximation of β-GPP/PPP networks for different α with $\beta = 1$.

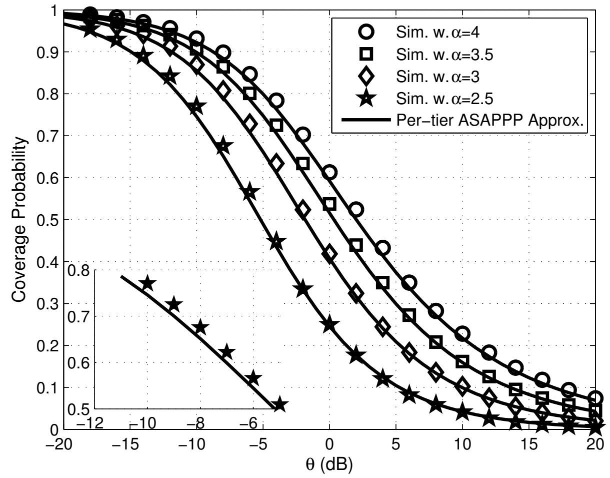

Fig. 5. The per-tier ASAPPP approximation of the square lattice/PPP networks for different α.

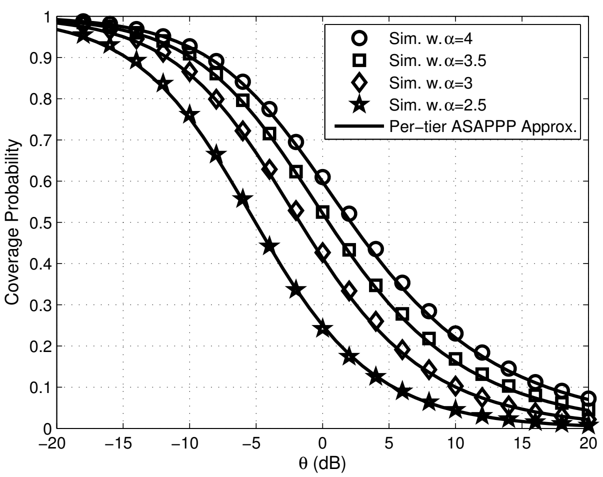

Fig. 6. The per-tier ASAPPP approximation of the two-tier GPP networks for different α.

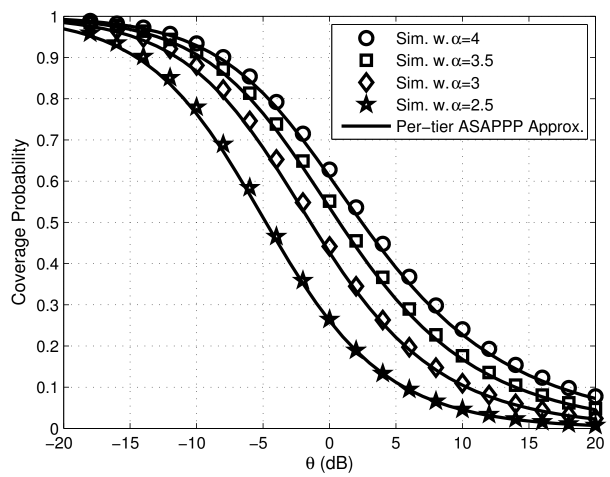

Fig. 7. The per-tier ASAPPP approximation of square lattice/GPP networks for different α.

HCNs relative to the PPP similar to the MISR-based gain based on the per-tier ASAPPP method such that the SIR distribution of HCNs can be approximated by shifting the curve of the PPP with the SIR gain.

When $\alpha_1 = \alpha_2 = \ldots = \alpha_k = \alpha$, letting $w_k \triangleq \frac{\lambda_k \mu_k^\delta}{\sum_{i\in[K]} \lambda_i \mu_i^\delta}$, we rewrite (15) as[5]

$$\hat{P}_{\rm c}(\theta) = \sum_{k\in[K]} w_k \frac{1}{w_k T(\alpha, \theta/G_k) + (1-w_k)\,T(\alpha,\theta)}. \quad (16)$$

Since $T(\alpha, \theta/G)$ is a convex function of $G \in (0, +\infty)$, a tight bound of (16) can be obtained. According to the definition of a convex function, we have

$$tT\left(\alpha, \frac{\theta}{G_1}\right) + (1-t)T\left(\alpha, \frac{\theta}{G_2}\right) \geq T\left(\alpha, \frac{\theta}{tG_1 + (1-t)G_2}\right).$$

[5]For the HIP model, w_k can be interpreted as the probability that the typical user is associated with a BS from tier k, which is consistent with the results concerning the association probability in [22] when the association bias is removed.

Therefore,

$$\hat{P}_{\rm c}(\theta) \leq \sum_{k\in[K]} w_k \frac{1}{T\left(\alpha, \frac{\theta}{w_k G_k + (1-w_k)}\right)}. \quad (17)$$

Since $\sum_{k\in[K]} w_k = 1$ and $1/T(\alpha, \theta/G)$ is a concave function of G, we obtain

$$\begin{aligned}\hat{P}_{\rm c}(\theta) &\leq \frac{1}{T\left(\alpha, \frac{\theta}{\sum_{k\in[K]} w_k(w_k G_k + (1-w_k))}\right)} \\ &= P_{\rm c}^{\rm PPP}\left(\frac{\theta}{\sum_{k\in[K]} w_k(w_k G_k + (1-w_k))}\right). \quad (18)\end{aligned}$$

By comparing the definition of the MISR-based gain with (18), we define the *effective gain* for K-tier HCNs as follows:

$$G_{\rm eff} \triangleq \sum_{k\in[K]} w_k(w_k G_k + (1-w_k))$$

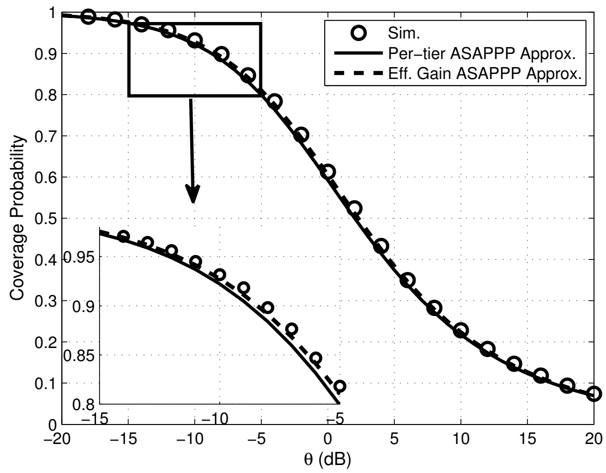

Fig. 8. Effective gain approximation for the coverage probability of square lattice/PPP deployment.

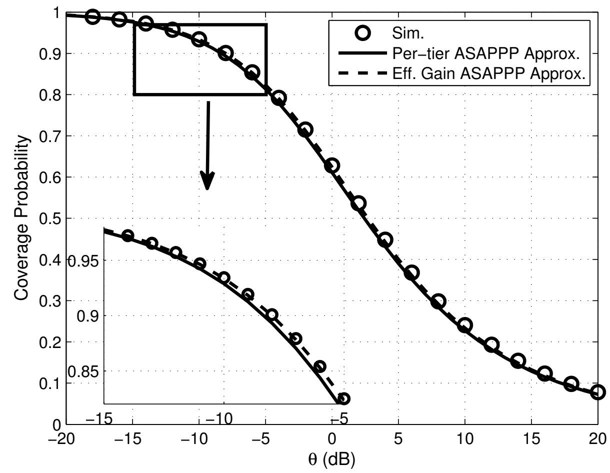

Fig. 9. Effective gain approximation for the coverage probability of square lattice/GPP deployment.

$$= \; 1+\sum_{k\in[K]} w_k^2(G_k-1). \tag{19}$$

Letting $\tilde{P}_{\rm c}(\theta) \triangleq P_{\rm c}^{\rm PPP}(\theta/G_{\rm eff})$, we know from (18) that the approximation by the effective gain method is an upper bound for that by the per-tier ASAPPP method in Section IV-A and gives a simpler expression, i.e., $\tilde{P}_{\rm c}(\theta) \geq \hat{P}_{\rm c}(\theta)$. The effective gain method establishes the relationship between the overall SIR gain of HCNs and individual MISR-based gains for the individual point processes constituting the HCNs. The effective gain for HCNs is equivalent to the MSIR-based gain for single-tier networks, which means the coverage probability of HCNs can be directly obtained by shifting the SIR threshold θ to $\theta/G_{\rm eff}$ from the coverage probability of the PPP. It should be noted that for the K-tier HIP model, $G_{\rm eff}\equiv 1$, which is consistent with the corresponding MISR-based gain. Further, for $G_k \geq 1, k\in[K]$, $G_{\rm eff} \leq \max\{G_k\}$ with equality only in the single-tier case.

Subtracting 1 from the gains, the effective gain can be compactly expressed as follows.

Corollary 2. *Defining $\tilde{G}_k \triangleq G_k-1$ and $\tilde{G}_{\rm eff} \triangleq G_{\rm eff}-1$, we obtain*

$$\tilde{G}_{\rm eff} = \sum_{k\in[K]} w_k^2 \tilde{G}_k. \tag{20}$$

One might think that the effective gain is simply the weighted average of the per-tier gains with weights w_k, i.e., an expected gain. However, this cannot hold since the superposition of many independent stationary point processes (under some mild technical conditions) yields a PPP. The following corollary gives a sufficient condition for the convergence of $\tilde{G}_{\rm eff} \to 0$ that is less restrictive than the one with identical tiers.

Corollary 3. *Let $\left(w_1^{(K)}, w_2^{(K)}, \cdots, w_K^{(K)}\right)$, $K\in\mathbb{N}$, be a sequence of probability mass functions, each corresponding to the values w_k in a K-tier network. If the probabilities $w_k^{(K)}$ satisfy $\lim\limits_{K\to\infty}\max\limits_{k\in[K]}\left\{\left(w_k^{(K)}\right)^2\right\}=0$, $G_{\rm eff}$ approaches 1 as $K\to\infty$, no matter what the G_k are.*

The proof is provided in Appendix A. It shows that $G_{\rm eff}\to 1$ under certain conditions, which is consistent with the fact that the superposition of K independent stationary point processes converges to a PPP as $K\to\infty$.

For example, according to [23, Theorem 1], the superposition of independent β-GPPs converges in distribution to a PPP, if the sequence $(c_k)_{k\in\mathbb{N}}$, $c_k\in\mathbb{R}_+$ is bounded and $\lim\limits_{K\to\infty} K^{-1}\sum_{k=1}^K c_k$ is finite and equal to c, each c_i relating to the density of a β-GPP with $\lambda_i = c_i/\pi$. These conditions are consistent with Corollary 2, i.e., $w_k^{(K)} = c_k/(\sum_{i=1}^K c_i)$ and $\lim\limits_{K\to\infty}\max\limits_{k\in[K]}\left\{\left(w_k^{(K)}\right)^2\right\} = 0$, which is proved in the following. Since $\lim\limits_{K\to\infty} K^{-1}\sum_{k=1}^K c_k = c$, $\forall\varepsilon>0$, $\exists M>0$, s.t. when $K>M$, we have $|K^{-1}\sum_{k=1}^K c_k - c| < \varepsilon$ and thus $\sum_{k=1}^K c_k > K(c-\varepsilon)$. Assume $c_i = \max\limits_{k\in[K]}\{c_k\}$ and thus the maximal probability is $w_i^{(K)} = c_i/(\sum_{k=1}^K c_k)$. We obtain

$$\begin{aligned}\left(w_i^{(K)}\right)^2 \;&=\; \left(\frac{c_i}{\sum_{k=1}^K c_k}\right)^2 < \left(\frac{c_i}{K(c-\varepsilon)}\right)^2 \\ &< \; \left(\frac{\hat{c}}{K(c-\varepsilon)}\right)^2 \overset{(d)}{<} \varepsilon,\end{aligned} \tag{21}$$

where $\hat{c}$ is an upper bound of $(c_k)_{k\in\mathbb{N}}$ and (d) holds when $K > \max\{M, \sqrt{1/\varepsilon}\left(\frac{\hat{c}}{c-\varepsilon}\right)^2\}$. Therefore, $\forall\varepsilon>0$, $\exists\widetilde{M} = \max\{M,\sqrt{1/\varepsilon}\left(\frac{\hat{c}}{c-\varepsilon}\right)^2\} > 0$, when $K>\widetilde{M}$, $\max\limits_{k\in[K]}\left\{\left(w_k^{(K)}\right)^2\right\} < \varepsilon$ and thus $\lim\limits_{K\to\infty}\max\limits_{k\in[K]}\left\{\left(w_k^{(K)}\right)^2\right\}=0$.

Table II gives the effective gains for some types of HCNs whose tiers have equal densities and transmit powers. Figure 8 and 9 show the coverage probability of two-tier heterogeneous networks comprising the square lattice/PPP and square lattice/GPP networks when $\lambda_1=\lambda_2=10^{-5}$, $\mu_1=\mu_2=1$ and $\alpha=4$. We also give two examples of 3-tier heterogeneous networks. Figure 10 and Figure 11 show the coverage probability of GPP/0.5-GPP/PPP and square lattice/GPP/PPP networks for different α, respectively. It is shown that both

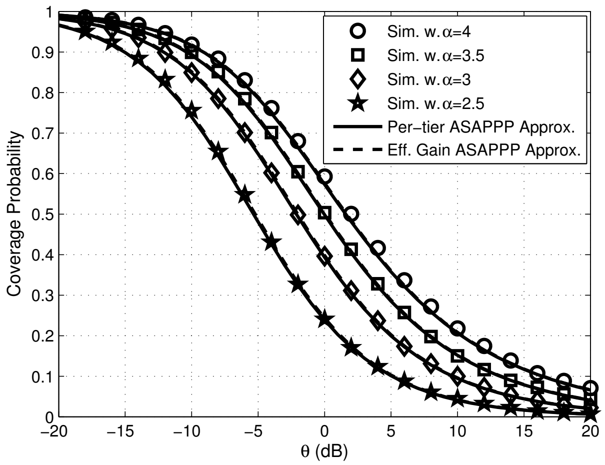

Fig. 10. The coverage probability of GPP/0.5-GPP/PPP networks for different α with $\lambda_1 = 10^{-5}$, $\mu_1 = 1$, $\lambda_2 = 2\lambda_1$, $\mu_2 = \mu_1/5$, $\lambda_3 = 5\lambda_1$ and $\mu_3 = \mu_1/25$.

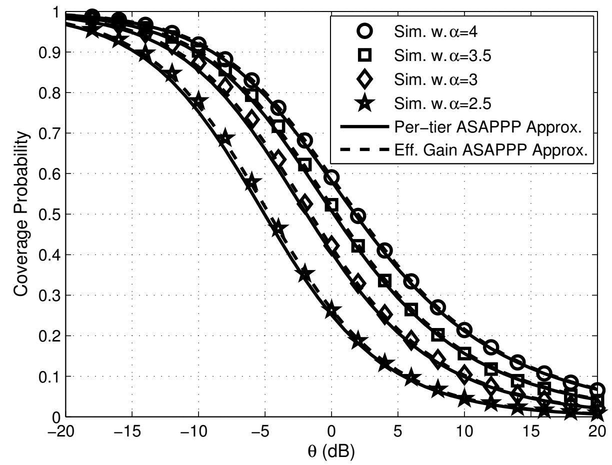

Fig. 11. The coverage probability of square lattice/GPP/PPP networks for different α with $\lambda_1 = 10^{-5}$, $\mu_1 = 1$, $\lambda_2 = 2\lambda_1$, $\mu_2 = \mu_1/5$, $\lambda_3 = 5\lambda_1$ and $\mu_3 = \mu_1/25$.

TABLE II. Effective gains for HCNs with tiers of equal densities and transmit powers

Two-tier HCNs	β-GPP/PPP	square lattice/PPP	β_1-GPP/β_2-GPP	square lattice/β-GPP
Effective Gain	1+β/8	1.25	1+$(\beta_1+\beta_2)$/8	1.25 + β/8
Three-tier HCNs	β_1-GPP/β_2-GPP/β_3-GPP		square lattice/β_1-GPP/β_2-GPP	
Effective Gain	1+$(\beta_1+\beta_2+\beta_3)$/18		1+$(\beta_1+\beta_2+2)$/18	
K-tier HCNs	each tier with the same MISR-based gain G			
Effective Gain	$1+(G-1)/K$			

per-tier and effective gain ASAPPP methods can approximate the simulation results in both two and three-tier HCNs cases, which demonstrates the effectiveness of the proposed methods for K-tier heterogeneous networks. We also observe that the effective gain method provides a closer approximation to the simulation results than the per-tier ASAPPP method.

E. Comparison of the two methods

We have established that the per-tier ASAPPP method provides an asymptotic lower bound to the exact results and is upper bounded by the effective gain method. Hence it is interesting to quantify how close the two are. Here, we will give an asymptotic comparison as $\theta \to 0$. According to the definition of the effective gain, we have

$$\tilde{F}(\theta) \triangleq 1 - \tilde{P}_{\rm c}(\theta) \sim \frac{\mathrm{MISR}_{\rm PPP}}{G_{\rm eff}}\theta, \quad \theta \to 0, \tag{22}$$

and according to the first-order Taylor expansion, we have

$$\hat{F}(\theta) \triangleq 1 - \hat{P}_{\rm c}(\theta) \sim -\hat{P}_{\rm c}'(0)\theta, \quad \theta \to 0, \tag{23}$$

where $\hat{P}_{\rm c}'(0)$ is the derivative of $\hat{P}_{\rm c}(\theta)$ at $\theta = 0$, given by

$$\hat{P}_{\rm c}'(\theta) = \sum_{k\in[K]} -w_k \frac{w_k T'(\alpha,\theta/G_k) + (1-w_k)T'(\alpha,\theta)}{\left(w_k T(\alpha,\theta/G_k) + (1-w_k)T(\alpha,\theta)\right)^2}, \tag{24}$$

where

$$T'\Big(\alpha, \frac{\theta}{G}\Big) = \frac{\delta}{G}\left(\Big(\frac{\theta}{G}\Big)^{\delta-1}\int_{\left(\frac{\theta}{G}\right)^{-\delta}}^{\infty} \frac{1}{1+t^{\alpha/2}}\mathrm{d}t + \frac{G}{\theta + G}\right).$$

Based on the L'Hôpital's rule, $T'(\alpha,\theta/G)|_{\theta=0} = \frac{2}{(\alpha-2)G}$ and we have

$$\begin{aligned}\hat{P}_{\rm c}'(0) &= -\frac{2}{\alpha-2}\sum_{k\in[K]} w_k(w_k/G_k + (1-w_k)) \\ &= -\mathrm{MISR}_{\rm PPP}\Big(1 + \sum_{k\in[K]} w_k^2(1/G_k - 1)\Big).\end{aligned} \tag{25}$$

Thus, the SIR gain $\hat{G}$ of the per-tier ASAPPP in K-tier HCNs relative to the PPP is given as

$$\begin{aligned}\hat{G} &\triangleq \frac{\mathrm{MISR}_{\rm PPP}}{-\hat{P}_{\rm c}'(0)} \\ &= \frac{1}{1 + \sum_{k\in[K]} w_k^2(1/G_k - 1)},\end{aligned} \tag{26}$$

and we call it *per-tier overall gain*. Consequently, the horizontal gap between the per-tier ASAPPP and the effective gain ASAPPP is given as

$$\begin{aligned} G_{\rm g} &\triangleq \frac{G_{\rm eff}}{\hat{G}} \\ &= \Big(1 + \sum_{k\in[K]} w_k^2(G_k - 1)\Big)\Big(1 + \sum_{k\in[K]} w_k^2(1/G_k - 1)\Big) \\ &= 1 + \Big(1 - \sum_{k\in[K]} w_k^2\Big)\sum_{k\in[K]} w_k^2(G_k + 1/G_k - 2) \\ &\quad + \sum_{\substack{i,j\in[K]\\ i<j}} w_i^2 w_j^2\left(\frac{G_i}{G_j} + \frac{G_j}{G_i} - 2\right) \\ &\geq 1, \end{aligned} \tag{27}$$

where the equality holds only in the case $G_k = 1, k \in [K]$, and thus we obtain $\tilde{P}_{\rm c}(\theta) \sim \hat{P}_{\rm c}(\theta/G_{\rm g}),\ \theta \to 0$. The reason why we call $G_{\rm eff}$ the effective gain is as follows: shifting the SIR distribution of Poisson networks with $\hat{G}$ has the same asymptotics as the per-tier ASAPPP and thus gives an asymptotically lower bound to the ccdf of the SIR, while the effective gain ASAPPP provides a tight upper bound for the per-tier ASAPPP and better approximates the SIR ccdfs, which can be observed from the results in Section IV-D.

V. The tail of the SIR distribution for HCNs

Similar to the asymptotic gain with $\theta \to 0$ in Section III, the gain G_∞ with $\theta \to \infty$ is used to characterize the tail asymptotics of the ccdf $\bar{F}_{\rm SIR}$ of the SIR in [14, 15] and defined as

$$G_\infty \triangleq \lim_{\theta\to\infty} G(\theta). \tag{28}$$

The *expected fading-to-interference ratio (EFIR)* is defined and plays a similar role for the gain with $\theta \to \infty$ as the MISR does for $\theta \to 0$. For a point process Φ with density λ, the EFIR is defined as

$$\mathrm{EFIR} \triangleq \left(\lambda\pi\mathbb{E}_o^!\left[\left(\frac{h}{I_\infty}\right)^\delta\right]\right)^{1/\delta}, \tag{29}$$

where $I_\infty \triangleq \sum_{x\in\Phi} h_x \ell(x)$, h is a fading random variable independent of all (h_x), and $\mathbb{E}_o^!$ is the expectation with respect to the reduced Palm measure of Φ. The EFIR for the PPP with arbitrary fading is given by $\mathrm{EFIR}_{\rm PPP} = (\mathrm{sinc}\,\delta)^{1/\delta}$. It is shown in [14, 15] that for an arbitrary stationary point process Φ with nearest-BS association,

$$P_{\rm c}(\theta) \sim \zeta\theta^{-\delta}, \quad \theta \to \infty, \tag{30}$$

where the pre-constant $\zeta = \mathrm{EFIR}^\delta$. It follows that the gain at $\theta \to \infty$ relative to the PPP is

$$G_\infty = \frac{\mathrm{EFIR}}{\mathrm{EFIR}_{\rm PPP}}. \tag{31}$$

Thus we call G_∞ EFIR-based gain, and we have $P_{\rm c}(\theta) \sim P_{\rm c}^{\rm PPP}(\theta/G_\infty),\ \theta \to \infty$. However, the complexity of heterogeneous networks prevents the straightforward application of the EFIR method for the tail of the SIR distribution for HCNs. Hence we explore whether the ASAPPP method depicted in Section III-B can be used to characterize the SIR tail of general HCNs. From [15, Lemma 7], the interference only affects the pre-constant on the tail of SIR distribution for all stationary point process and arbitrary fading. Therefore, we investigate how to use G_∞^k for the individual tiers to estimate the pre-constant ζ using the ASAPPP method, where G_∞^k is the k-th tier EFIR-based gain of K-tier HCNs.

Theorem 2. *Let*

$$\hat{P}_{\rm c}(\theta) \triangleq \sum_{k\in[K]} \lambda_k\pi\theta^{-\delta_k}\mathbb{E}(h^{\delta_k})\mathbb{E}\left[\left(\frac{I_k^{\rm PPP}}{G_\infty^k} + \sum_{i\in[K]^!}\frac{\mu_i}{\mu_k}I_i^{\rm PPP}\right)^{-\delta_k}\right],$$

where $I_k^{\rm PPP} \triangleq \sum_{x\in\Phi_k^{\rm PPP}} h_x|x|^{-\alpha_k}$ and the $\Phi_k^{\rm PPP}$ are independent PPPs with densities λ_k. For K-tier HCNs where the typical user is served by the BS with the strongest average received power, the coverage probability $P_{\rm c}(\theta)$ is asymptotically lower bounded by

$$P_{\rm c}(\theta) \gtrsim \hat{P}_{\rm c}(\theta), \quad \theta \to \infty. \tag{32}$$

The proof is provided in Appendix B. Since the asymptote is obtained using the EFIR-based gains for each individual tier with the ASAPPP method, we call it per-tier ASAPPP asymptote at infinity. As before, we obtain a simplified expression when the path loss exponents are all equal.

Corollary 4. *When $\alpha_1 = \ldots = \alpha_k = \alpha$, let*

$$\hat{\zeta} \triangleq \sum_{k\in[K]} \frac{\lambda_k\mu_k^\delta\mathrm{sinc}\,\delta}{\lambda_k(\mu_k/G_\infty^k)^\delta + \sum_{i\in[K]^!}\lambda_i\mu_i^\delta}. \tag{33}$$

The pre-constant ζ of the K-tier HCNs is $\zeta \gtrsim \hat{\zeta}$, i.e., $P_{\rm c}(\theta) \gtrsim \hat{\zeta}\theta^{-\delta}$, $\theta \to \infty$, and the per-tier overall gain at infinity is $\hat{G}_\infty = \hat{\zeta}^{1/\delta}/\mathrm{EFIR}_{\rm PPP}$.

Proof: When $\alpha_1 = \ldots = \alpha_k = \alpha$,

$$\begin{aligned}
&\mathbb{E}\left\{\left(\frac{I_k^{\rm PPP}}{G_\infty^k} + \sum_{i\in[K]^!}\frac{\mu_i}{\mu_k}I_i^{\rm PPP}\right)^{-\delta}\right\}\\
&= \frac{1}{\Gamma(\delta)}\int_0^\infty \mathcal{L}_{I_k^{\rm PPP}}(s/G_\infty^k)\prod_{i\in[K]^!}\mathcal{L}_{I_i^{\rm PPP}}(\mu_i s/\mu_k)s^{-1+\delta}\mathrm{d}s\\
&= \frac{1}{\Gamma(\delta)}\int_0^\infty \exp\Bigg(-\pi\mathbb{E}(h^\delta)\Gamma(1-\delta)s^\delta\\
&\qquad\times\left(\sum_{i\in[K]^!}\lambda_i\left(\frac{\mu_i}{\mu_k}\right)^\delta + \frac{\lambda_k}{(G_\infty^k)^\delta}\right)\Bigg)s^{-1+\delta}\mathrm{d}s\\
&= \frac{\mu_k^\delta\mathrm{sinc}\,\delta}{\pi\mathbb{E}(h^\delta)\left(\lambda_k(\mu_k/G_\infty^k)^\delta + \sum_{i\in[K]^!}\lambda_i\mu_i^\delta\right)}
\end{aligned} \tag{34}$$

because $I^{-\delta} \equiv \frac{1}{\Gamma(\delta)}\int_0^\infty e^{-sI}s^{-1+\delta}\mathrm{d}s$. Thus

$$P_{\rm c}(\theta) \gtrsim \theta^{-\delta}\sum_{k\in[K]} \frac{\lambda_k\mu_k^\delta\mathrm{sinc}\,\delta}{\lambda_k(\mu_k/G_\infty^k)^\delta + \sum_{i\in[K]^!}\lambda_i\mu_i^\delta}, \quad \theta \to \infty. \tag{35}$$

■

As for the derivation of the effective gain at zero in Section IV-D, we can rewrite (33) as

$$\begin{aligned}
\hat{\zeta} &= \sum_{k\in[K]} w_k\frac{\mathrm{sinc}\,\delta}{w_k(G_\infty^k)^{-\delta} + 1 - w_k}\\
&\le \mathrm{sinc}\,\delta\sum_{k\in[K]} w_k(w_kG_\infty^k + 1 - w_k)^\delta\\
&\le \mathrm{sinc}\,\delta\Big(\sum_{k\in[K]} w_k(w_kG_\infty^k + 1 - w_k)\Big)^\delta,
\end{aligned} \tag{36}$$

because $G^{-\delta}$ and G^δ are convex and concave functions of G, respectively. Compared with the definition of the EFIR-based gain in (30) and (31), we also define the effective gain for HCNs as $\theta \to \infty$, given by

$$G_\infty^{\rm eff} = \sum_{k\in[K]} w_k(w_kG_\infty^k + 1 - w_k)$$

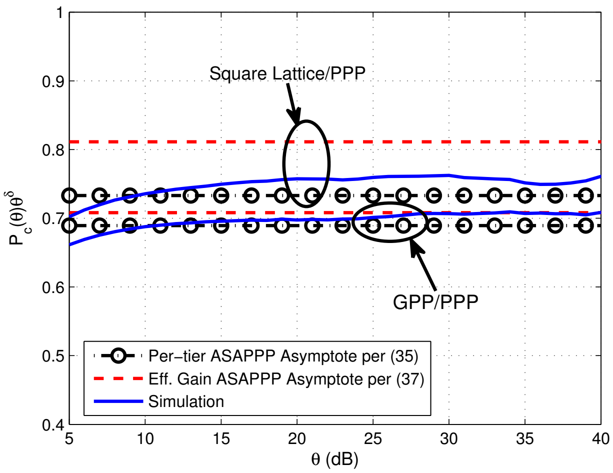

Fig. 12. Scaled coverage probability $P_c(\theta)\theta^\delta$ per (35) and (37) for non-Poisson/PPP networks with $\alpha = 4$, $\lambda_1 = \lambda_2 = 10^{-5}$ and $\mu_1 = \mu_2 = 1$.

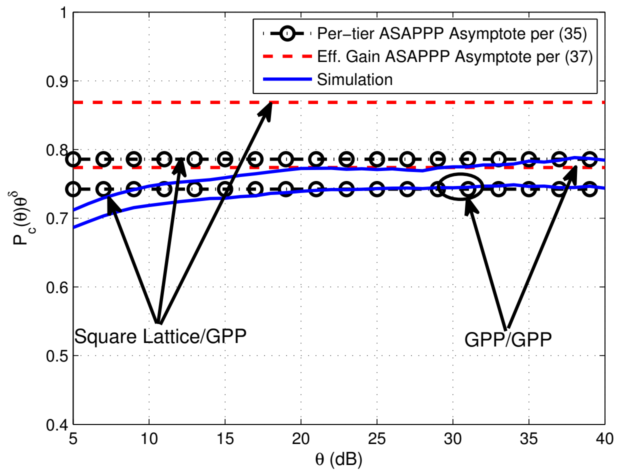

Fig. 13. Scaled coverage probability $P_c(\theta)\theta^\delta$ per (35) and (37) for non-Poisson/non-Poisson networks with $\alpha = 4$, $\lambda_1 = \lambda_2 = 10^{-5}$ and $\mu_1 = \mu_2 = 1$.

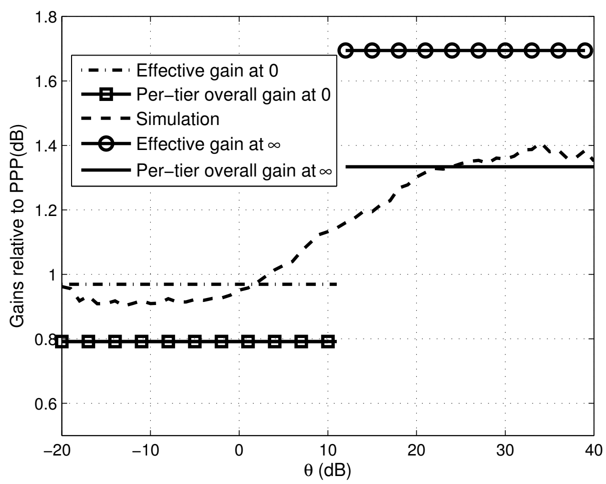

Fig. 14. Gains $G(\theta)$ for GPP/GPP networks with $\alpha = 4$, $\lambda_1 = \lambda_2 = 10^{-5}$ and $\mu_1 = \mu_2 = 1$.

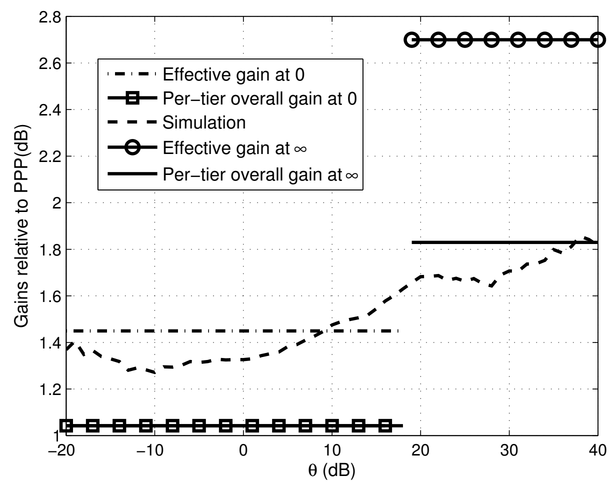

Fig. 15. Gains $G(\theta)$ for square lattice/GPP networks with $\alpha = 4$, $\lambda_1 = \lambda_2 = 10^{-5}$ and $\mu_1 = \mu_2 = 1$.

$$= 1 + \sum_{k\in[K]} w_k^2 (G_\infty^k - 1). \tag{37}$$

The asymptote is obtained using the effective gain at infinity with the ASAPPP method, and thus we call it effective gain ASAPPP asymptote. As for the gain at 0 in Corollary 2, this can be written more compactly.

Corollary 5. *Defining* $\tilde{G}_\infty^k \triangleq G_\infty^k - 1$ *and* $\tilde{G}_\infty^{\rm eff} \triangleq G_\infty^{\rm eff} - 1$, *we obtain*

$$\tilde{G}_\infty^{\rm eff} = \sum_{k\in[K]} w_k^2 \tilde{G}_\infty^k. \tag{38}$$

$G_\infty^{\rm eff}$ has the same expression as $G_{\rm eff}$, which is again in agreement with the fact that the superposition of many independent stationary point processes yields a PPP under certain conditions. According to [15], the EFIRs of the square lattice and GPP with $\alpha = 4$ are 1.42 and 0.80, respectively. Therefore, the corresponding EFIR-based gains are 3.49 and 1.95, respectively. Figure 12 and 13 show the scaled coverage probability $P_c(\theta)\theta^\delta$ of the heterogeneous networks comprising non-Poisson/PPP and non-Poisson/non-Poisson networks, respectively. Since the approximations are obtained by the asymptotic gains at ∞, we focus on the range of relatively large θ. It can be observed that the per-tier ASAPPP asymptote provides a closer approximation than the effective gain ASAPPP asymptote except for GPP/PPP networks while the per-tier ASAPPP asymptote also approximates the simulation results well in GPP/PPP networks. When $\theta > 15$ dB for non-Poisson/PPP networks and $\theta > 20$ dB for non-Poisson/non-Poisson networks, the coverage probability is quite close to the per-tier ASAPPP asymptotes.

Figure 14 and 15 show the gains as a function of θ and the effective gains and per-tier overall gains at 0 and ∞ for the GPP/GPP and square lattice/GPP networks, respectively. It is observed that the gain is larger than the per-tier overall gain at 0 and smaller than the effective gain at infinity. We also observe that the gains for the two types of networks are not monotone, first decrease and then increase similar to the single-tier case illustrated in [15, Fig. 7]. As $\theta \to 0$, the gains approximate the effective gains at zero and are larger than the corresponding per-tier overall gains. As $\theta \to \infty$, the gains approximate the per-tier overall gains at infinity and are smaller than the corresponding effective gains, and the approximation provided by the per-tier overall gain is highly accurate at infinity. From the above discussion, it is interesting to determine a demarcation of the SIR threshold $\theta_{\rm d}$ such that $G(\theta) \approx G_{\rm eff}$ if $\theta < \theta_{\rm d}$, otherwise $G(\theta) \approx \hat{G}_\infty$. Letting $P_{\rm c1}(\theta) = P_{\rm c}^{\rm PPP}(\theta/G_{\rm eff})$ and $P_{\rm c2}(\theta) = P_{\rm c}^{\rm PPP}(\theta/\hat{G}_\infty)$, $\theta_{\rm d}$ is obtained by minimizing the following metric

$$E(\theta_{\rm d})=\int_a^{\theta_{\rm d}}\big(P_{\rm c}(t)-P_{\rm c1}(t)\big)^2{\rm d}t+\int_{\theta_{\rm d}}^b\big(P_{\rm c}(t)-P_{\rm c2}(t)\big)^2{\rm d}t, \quad (39)$$

where $a,\ b \in \mathbb{R}$, t is the SIR threshold in dB, and $P_{\rm c}(t)$ is the actual coverage probability. Using this approach, when $a = -20$ dB and $b = 40$ dB, we obtain $\theta_{\rm d} = 11.65$ dB and 18.35 dB in Figure 14 and 15, respectively.

VI. Exact Analysis of β-GPP/PPP HCNs

In [10, 24, 25], the authors derived the coverage probability for the typical user associated with the BS that offers the strongest average received power. However, an explicit derivation for the coverage performance of HCNs based on the β-GPP and PPP is still missing in the literature, and Section IV-B1 only gives the ASAPPP-based approximations. Therefore, in this section we derive the exact coverage performance for this type of HCNs and compare it with the approximative approaches. Assume that the locations of the MBSs Φ_1 are modeled by a β-GPP, and the locations of the PBSs Φ_2 are modeled by a PPP. The following theorem gives the exact coverage probability for the typical user with the strongest-BS association in the β-GPP/PPP deployment.

Theorem 3. *When the user accesses an MBS, we have*

$$P_{\rm m}(\theta)=\beta\sum_{k\in\mathbb{N}}\int_0^\infty\frac{r^{k-1}e^{-r}}{\Gamma(k)}\prod_{i\in\mathbb{N}\setminus\{k\}}\Bigg(1-\beta+\beta\int_r^\infty\frac{t^{i-1}e^{-t}}{\Gamma(i)\left(1+\theta\left(\frac{r}{t}\right)^{\alpha/2}\right)}{\rm d}t\Bigg)e^{-\omega\beta T(\alpha,\theta)r}{\rm d}r. \quad (40)$$

When the user accesses a PBS, we have

$$P_{\rm p}(\theta)=\int_0^\infty\prod_{i\in\mathbb{N}}\Bigg(1-\beta+\beta\int_{\frac{r}{\omega\beta}}^\infty\frac{t^{i-1}e^{-t}}{\Gamma(i)\left(1+\frac{\theta r^{\alpha/2}}{(\omega\beta t)^{\alpha/2}}\right)}{\rm d}t\Bigg)e^{-T(\alpha,\theta)r}{\rm d}r. \quad (41)$$

By substituting (40) and (41) into (2), we obtain the coverage probability.

The proof is provided in Appendix C. The complexity of (40) is the same as the single-tier β-GPP result [5], and (41) is simpler with just two infinite integrals and one infinite product due to the tractability of the PPP. According to [25, Lemma 3 and 4], we can straightforwardly obtain asymptotics of (40) and (41) as $\theta \to \infty$, given by

$$P_{\rm m}(\theta)\sim\theta^{-\delta}\int_0^\infty\prod_{i=2}^\infty\Bigg(1-\beta+\beta\int_0^\infty\frac{t^{i-1}e^{-t}}{\Gamma(i)\left(1+\frac{r^{\alpha/2}}{(\beta t)^{\alpha/2}}\right)}{\rm d}t\Bigg)e^{-\frac{\omega r}{\operatorname{sinc}\delta}}{\rm d}r, \quad (42)$$

$$P_{\rm p}(\theta)\sim\theta^{-\delta}\int_0^\infty\prod_{i=1}^\infty\Bigg(1-\beta+\beta\int_0^\infty\frac{t^{i-1}e^{-t}}{\Gamma(i)\left(1+\frac{r^{\alpha/2}}{(\beta t)^{\alpha/2}}\right)}{\rm d}t\Bigg)e^{-\frac{\omega r}{\operatorname{sinc}\delta}}\omega{\rm d}r. \quad (43)$$

From the proof of [25, Proposition 5], we obtain

$$\prod_{i=2}^\infty\Bigg(1-\beta+\beta\int_0^\infty\frac{t^{i-1}e^{-t}}{\Gamma(i)\left(1+(r/(\beta t))^{\alpha/2}\right)}{\rm d}t\Bigg)\sim\exp\Big(-\frac{r}{\operatorname{sinc}\delta}\Big)$$

as $\beta \to 0$. Therefore, when $\beta \to 0$,

$$P_{\rm m}(\theta)\sim\theta^{-\delta}\frac{\lambda_1\mu_1^\delta}{\lambda_1\mu_1^\delta+\lambda_2\mu_2^\delta}\operatorname{sinc}\delta, \quad \theta\to\infty, \quad (44)$$

$$P_{\rm p}(\theta)\sim\theta^{-\delta}\frac{\lambda_2\mu_2^\delta}{\lambda_1\mu_1^\delta+\lambda_2\mu_2^\delta}\operatorname{sinc}\delta, \quad \theta\to\infty. \quad (45)$$

Consequently, when $\beta \to 0$, $P_{\rm c}(\theta) = P_{\rm m}(\theta) + P_{\rm p}(\theta) \sim \theta^{-\delta}\operatorname{sinc}\delta$, $\theta \to \infty$, which is consistent with the asymptotic behavior in Poisson networks.

Figure 16 compares the theoretical results and the effective gain ASAPPP approximations for different α, and Figure 17 compares the theoretical asymptote and ASAPPP asymptotes when $\beta = 1$, $\lambda_1 = 10^{-5}$, $\mu_1 = 1$, $\lambda_2 = 2\lambda_1$ and $\mu_2 = \mu_1/25$. We observe that the effective gain ASAPPP and ASAPPP asymptotes approximate theoretical results quite well. From the expressions of the theoretical and approximative results, the ASAPPP method avoids the numerical computation of infinite sum, product and integral and thus the results can be obtained much more efficiently. For Figure 16, it takes about 600s to calculate one point of the theoretical curves for $\alpha = 4$, 3.5 and 3, while in the case $\alpha = 2.5$, about 25 hours are needed to calculate one point of the theoretical curve with Matlab2014b[6], because more items (inner integrals for different i) in the infinite sum and product part should be calculated to avoid the truncation error (50000 items are needed in our results for $\alpha = 2.5$ and 500 items are needed for $\alpha = 4$, 3.5 and 3). However, it takes only about 0.03s to calculate one point in the approximative curves with the help of hypergeometric functions in Matlab. The speed-up from using ASAPPP is about four orders of magnitude and even larger when $\alpha = 2.5$. Consequently, the above discussion demonstrates the effectiveness of the ASAPPP-based approximations for their simplicity and acceptable accuracy.

VII. Conclusions

In this paper, we provided simple approximative approaches to the SIR analysis in general K-tier HCNs based on the MISR-based gain for each individual tier. We first established the per-tier ASAPPP-based approximation for general K-tier

[6]The results are obtained on a Mac equipped with 3 GHz Intel core i7 processors.

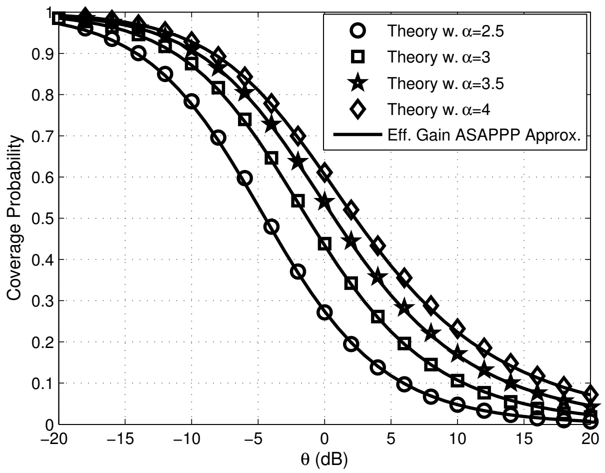

Fig. 16. Exact and approximative coverage probabilities of GPP/PPP networks for different α when $\lambda_2 = 2\lambda_2$ and $\mu_1 = 25\mu_2$.

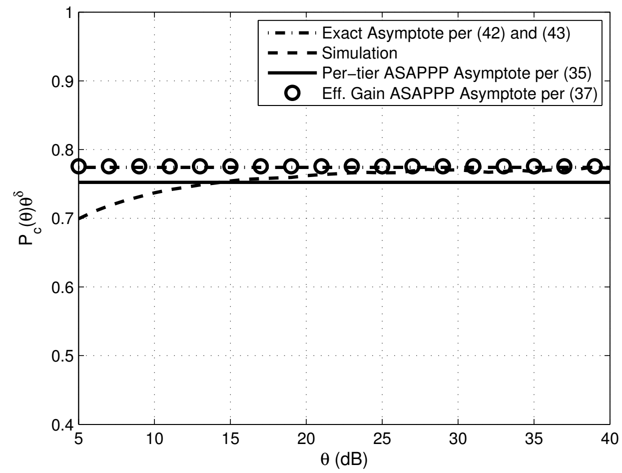

Fig. 17. Scaled coverage probability $P_{\rm c}(\theta)\theta^{\delta}$ per (35), (37), (42) and (43) for GPP/PPP networks with $\alpha = 4$, $\lambda_2 = 2\lambda_1$ and $\mu_1 = 25\mu_2$.

HCNs, and then an alternative approach is inspired by the per-tier ASAPPP method with an explicit expression for the effective gain $G_{\rm eff}$ of HCNs such that $P_{\rm c}^{\rm HCN}(\theta) \approx P_{\rm c}^{\rm PPP}(\theta/G_{\rm eff})$ when the path loss exponents are the same for all tiers. We found that the effective gain at zero lies in between the tier with the largest MISR-based gain and the Poisson networks due to the independence among different tiers. Furthermore, we gave the approximative asymptote for the tail of the SIR distribution using the ASAPPP method. The expression of the effective gain at infinity is the same as the one at zero. The effective gains at both infinity and zero approach 1 as K grows (under certain conditions), which is consistent with the fact the superposition of many independent stationary point processes yields a PPP. Besides, to highlight the simplicity and effectiveness of approximative approaches, we compare the approximative and exact SIR distributions in terms of accuracy and efficiency in the two-tier HCNs modeled by β-Ginibre and Poisson point processes. The results indicate that the ASAPPP method gives simple yet close approximations to the SIR distribution over a wide range of SIR thresholds, thus providing a useful approach for practical network models where an exact calculation of the SIR distribution is unfeasible or very hard.

Appendix A
Proof of Corollary 3

We first prove that when $\lim\limits_{K\to\infty} \max\limits_{k\in[K]} \left\{ \big(w_k^{(K)}\big)^2 \right\} = 0$, $\lim\limits_{K\to\infty} \sum\limits_{k\in[K]} \big(w_k^{(K)}\big)^2 = 0$ holds. We assume $\max\limits_{k\in[K]}\{w_k^{(K)}\} = w_i^{(K)}$ and thus $w_i^{(K)} \geq 1/K$. According to the definition of a limit, $\forall\varepsilon > 0$ and $\varepsilon < 1$, $\exists M > 0$, s.t. when $K > M$, we have $\big(w_k^{(K)}\big)^2 < \varepsilon^2 < 1, k \in [K]$ and thus $w_k^{(K)} < \varepsilon$. Letting $\widetilde{M} = \max\{M, 1/\varepsilon\} > 0$, when $K > \widetilde{M}$, we have $w_i^{(K)} \in [1/K,\ \varepsilon)$. Then, for any $i \in [K]$,

$$\sum_{k\in[K]} \big(w_k^{(K)}\big)^2 = 1 - w_i^{(K)}\big(1 - w_i^{(K)}\big) - \sum_{\substack{k\in[K]\\k\neq i}} w_k^{(K)}\big(1 - w_k^{(K)}\big)$$

$$< 1 - w_i^{(K)}\big(1 - w_i^{(K)}\big) - \sum_{\substack{k\in[K]\\k\neq 1}} w_k^{(K)}(1-\varepsilon)$$
$$= \big(w_i^{(K)}\big)^2 + \varepsilon\big(1 - w_i^{(K)}\big) \overset{(a)}{<} \varepsilon. \tag{46}$$

Step (a) holds because when $K > \widetilde{M}$, it is obtained that the maximum of the quadratic function with respect to $w_i^{(K)}$ in (46) is achieved at $w_i^{(K)} = \varepsilon$. Therefore, $\forall\varepsilon > 0$, $\exists\widetilde{M} > 0$, s.t. when $K > \widetilde{M}$, we have $\sum\limits_{k\in[K]} \big(w_k^{(K)}\big)^2 < \varepsilon$. Accordingly, we obtain $\lim\limits_{K\to\infty} \sum\limits_{k\in[K]} \big(w_k^{(K)}\big)^2 = 0$.

Second, we prove $\lim\limits_{K\to\infty} \tilde{G}_{\rm eff} = 0$, no matter what the G_k are. We denote the maximum and minimum of $\tilde{G}_k$ as $\tilde{G}_{\max}$ and $\tilde{G}_{\min}$, respectively. Since $\tilde{G}_{\min} \sum\limits_{k\in[K]} \big(w_k^{(K)}\big)^2 \leq \tilde{G}_{\rm eff} \leq \tilde{G}_{\max} \sum\limits_{k\in[K]} \big(w_k^{(K)}\big)^2$ and G_k is bounded[7], e.g., $\tilde{G}_{\max} < 2$, $\lim\limits_{K\to\infty} \tilde{G}_{\rm eff} = 0$ holds, and $G_{\rm eff}$ approaches 1.

Appendix B
Proof of Theorem 2

As before, we express the coverage probability $P_{\rm c}(\theta)$ as the total probability of the disjoint events that the typical user accesses a BS from tier k, i.e.,

$$P_{\rm c}(\theta) = \sum_{k\in[K]} \mathbb{P}(\mathrm{SIR} > \theta, x_0 \in \Phi_k). \tag{47}$$

Defining $R \triangleq |x_0|$, we obtain

$$\begin{aligned}
&\mathbb{P}(\mathrm{SIR} > \theta, x_0 \in \Phi_k)\\
&= \mathbb{E}\left\{ \frac{\mu_k R^{-\alpha_k} h \mathbf{1}_{x_0\in\Phi_k}}{\sum\limits_{x\in\Phi_k^!} \mu_k |x|^{-\alpha_k} h_x + \sum\limits_{i\in[K]^!} \sum\limits_{y\in\Phi_i} \mu_i |y|^{-\alpha_i} h_y} > \theta \right\}\\
&= \mathbb{E}\left\{ \bar{F}_h(\theta R^{\alpha_k} I) \mathbf{1}_{x_0\in\Phi_k} \right\},
\end{aligned} \tag{48}$$

[7]The triangular lattice (which has hexagonal cells) has the maximal gain 3.4 dB, i.e., $\tilde{G}_{\rm tri} \approx 1.2$ [6].

where $I = \sum_{x\in\Phi_k^!} \mu_k|x|^{-\alpha_k}h_x + \sum_{i\in[K]^!}\sum_{y\in\Phi_i}\mu_i|y|^{-\alpha_i}h_y$. Letting $\mathcal{C}_k(x) = \{\Phi_k(b(o,|x|) = 0)\}$, $\mathcal{D}_{i,k}(x) = \{\Phi_i(b(o,(\mu_i/\mu_k)^{1/\alpha_i}|x|^{\alpha_k/\alpha_i})) = 0)\}$, and using the representation [15, Eqn. 18] and following the Campbell-Mecke theorem [21, Thm. 8.2], the coverage probability of the user accessing a BS from the k-tier can be expressed as

$$\begin{aligned}
&\mathbb{P}(\mathrm{SIR}>\theta, x_0\in\Phi_k)\\
&=\mathbb{E}\sum_{x\in\Phi_k}\bar{F}_h\Bigg[\theta|x|^{\alpha_k}\Bigg(\sum_{y\in\Phi_k^!}|y|^{-\alpha_k}h_x\\
&\qquad+\sum_{i\in[K]^!}\sum_{y\in\Phi_i}\frac{\mu_i}{\mu_k}|y|^{-\alpha_i}h_y\Bigg)\Bigg]\mathbf{1}_{\mathcal{C}_k(x)}\prod_{i\in[K]^!}\mathbf{1}_{\mathcal{D}_{i,k}(x)}\\
&=\lambda_k\int_{\mathbb{R}^2}\mathbb{E}^{!k}\Bigg\{\bar{F}_h\Bigg[\theta|x|^{\alpha_k}\Bigg(\sum_{y\in\Phi_k^x}|y|^{-\alpha_k}h_y\\
&\qquad+\sum_{i\in[K]^!}\sum_{y\in\Phi_i}\frac{\mu_i}{\mu_k}|y|^{-\alpha_i}h_y\Bigg)\Bigg]\mathbf{1}_{\mathcal{C}_k(x)}\prod_{i\in[K]^!}\mathbf{1}_{\mathcal{D}_{i,k}(x)}\Bigg\}\mathrm{d}x\\
&\overset{(a)}{\sim}\lambda_k\int_{\mathbb{R}^2}\mathbb{E}^{!k}\Bigg\{\bar{F}_h\Bigg(\frac{\theta}{G_\infty^k}|x|^{\alpha_k}\sum_{y\in\Phi_{k,\mathrm{PPP}}^x}|y|^{-\alpha_k}h_y\\
&\qquad+\theta|x|^{\alpha_k}\sum_{i\in[K]^!}\sum_{y\in\Phi_i}\frac{\mu_i}{\mu_k}|y|^{-\alpha_i}h_y\Bigg)\mathbf{1}_{\mathcal{C}_k(x)}\prod_{i\in[K]^!}\mathbf{1}_{\mathcal{D}_{i,k}(x)}\Bigg\}\mathrm{d}x\\
&\overset{(b)}{\gtrsim}\lambda_k\int_{\mathbb{R}^2}\mathbb{E}^{!k}\Bigg\{\bar{F}_h\Bigg[\theta|x|^{\alpha_k}\Bigg(\frac{1}{G_\infty^k}\sum_{y\in\Phi_{k,\mathrm{PPP}}^x}|y|^{-\alpha_k}h_y\\
&\qquad+\sum_{i\in[K]^!}\sum_{y\in\Phi_i^{\mathrm{PPP}}}\frac{\mu_i}{\mu_k}|y|^{-\alpha_i}h_y\Bigg)\Bigg]\mathbf{1}_{\mathcal{C}_k(x)}\prod_{i\in[K]^!}\mathbf{1}_{\mathcal{D}_{i,k}(x)}\Bigg\}\mathrm{d}x
\end{aligned}\tag{49}$$

as $\theta\to\infty$, where $\Phi^x \triangleq \{y\in\Phi : y+x\}$ is a translated version of Φ and $\mathbb{E}^{!k}$ is the expectation with respect to Φ_i, $i\in[K]^!$, and the reduced Palm measure of Φ_k. Step (a) uses the asymptotically exact ASAPPP approximation of Φ_k by shifting θ to θ/G_∞^k as $\theta\to\infty$ and replacing Φ_k by a PPP [15]. In step (b) the interference from Φ_i is upper bounded by that of a PPP. Substituting $x\theta^{\delta/2}\mapsto x$ and letting $I_k = \sum_{x\in\Phi_k} h_x|x|^{-\alpha_k}$,

$$\begin{aligned}
&\mathbb{P}(\mathrm{SIR}>\theta, x_0\in\Phi_k)\\
&\gtrsim\lambda_k\theta^{-\delta_k}\int_{\mathbb{R}^2}\mathbb{E}^{!k}\Bigg\{\bar{F}_h\Bigg(|x|^{\alpha_k}\Bigg(\frac{I_k^{\mathrm{PPP}}}{G_\infty^k}+\sum_{i\in[K]^!}\frac{\mu_i}{\mu_k}I_i^{\mathrm{PPP}}\Bigg)\Bigg)\\
&\qquad\times\mathbf{1}_{\mathcal{C}_k(\theta^{-\delta_k/2}x)}\prod_{i\in[K]^!}\mathbf{1}_{\mathcal{D}_{i,k}(\theta^{-\delta_k/2}x)}\Bigg\}\mathrm{d}x\\
&\overset{(c)}{\sim}\lambda_k\theta^{-\delta_k}\int_{\mathbb{R}^2}\mathbb{E}^{!k}\Bigg\{\bar{F}_h\Bigg(|x|^{\alpha_k}\Bigg(\frac{I_k^{\mathrm{PPP}}}{G_\infty^k}+\sum_{i\in[K]^!}\frac{\mu_i}{\mu_k}I_i^{\mathrm{PPP}}\Bigg)\Bigg)\Bigg\}\mathrm{d}x\\
&\sim\lambda_k\theta^{-\delta_k}\mathbb{E}^{!k}\Bigg\{\Bigg(\frac{I_k^{\mathrm{PPP}}}{G_\infty^k}+\sum_{i\in[K]^!}\frac{\mu_i}{\mu_k}I_i\Bigg)^{-\delta_k}\Bigg\}\int_{\mathbb{R}^2}\bar{F}_h(|x|^{\alpha_k})\mathrm{d}x\\
&\sim\lambda_k\pi\theta^{-\delta_k}\mathbb{E}(h^{\delta_k})\mathbb{E}^{!k}\Bigg\{\Bigg(\frac{I_k^{\mathrm{PPP}}}{G_\infty^k}+\sum_{i\in[K]^!}\frac{\mu_i}{\mu_k}I_i\Bigg)^{-\delta_k}\Bigg\}\\
&\overset{(d)}{\sim}\lambda_k\pi\theta^{-\delta_k}\mathbb{E}(h^{\delta_k})\mathbb{E}\Bigg\{\Bigg(\frac{I_k^{\mathrm{PPP}}}{G_\infty^k}+\sum_{i\in[K]^!}\frac{\mu_i}{\mu_k}I_i\Bigg)^{-\delta_k}\Bigg\},
\end{aligned}\tag{50}$$

where (c) follows since $\theta^{-\delta_k/2}\to 0$ and hence $\mathbf{1}_{\mathcal{C}_k(\theta^{-\delta_k/2}x)}\to 1$ and $\mathbf{1}_{\mathcal{D}_{i,k}(\theta^{-\delta_k/2}x)}\to 1$, and (d) holds since $\mathbb{E}_o^! = \mathbb{E}$ for the PPP.

Appendix C
Proof of Theorem 3

We know that the distance between a user and its nearest PBS is distributed as $f(r) = 2\pi\lambda_2 re^{-\lambda_2\pi r^2}$. Letting $c=\pi\lambda_1$, the squared moduli of the distances between the user and the MBSs have the same distribution as the set of random variables obtained by retaining the gamma variables $Q_k\sim\mathrm{gamma}(k,\beta/c)$, $k\in\mathbb{N}$, with probability β independently (details in the Proposition 1 in [5]). For simplicity, we use a family of independent indicators (T_i) with $\mathbb{E}T_i=\beta$, $T_i\in\{0,1\}$ to indicate whether the gamma variables are retained. As before, the coverage probability is expressed as the total probability of the typical user being served by a BS from different tiers. When the user accesses an MBS, i.e., $\mu_1\ell(x_0)>\mu_2\ell(y)$, where $x_0\in\Phi_1$ and $y\in\Phi_2$, we have

$$\begin{aligned}
&P_{\mathrm{m}}(\theta)=\mathbb{P}(\mathrm{SIR}>\theta, x_0\in\Phi_1)\\
&=\mathbb{E}\Bigg\{\exp\Bigg(-\frac{\theta}{\mu_1\ell(x_0)}\Bigg(\sum_{x\in\Phi_1^!}\mu_1\ell(x)h_x+\sum_{y\in\Phi_2}\mu_2\ell(y)h_y\Bigg)\Bigg)\mathbf{1}_{x_0\in\Phi_1}\Bigg\}\\
&=\mathbb{E}\Bigg\{\prod_{x\in\Phi_1^!}\Bigg(1+\frac{\theta\ell(x)}{\ell(x_0)}\Bigg)^{-1}\mathbf{1}_{\{|x|\geq|x_0|\}}\prod_{y\in\Phi_2}\Bigg(1+\frac{\theta\mu_2\ell(y)}{\mu_1\ell(x_0)}\Bigg)^{-1}\mathbf{1}_{\{|y|\geq\eta|x_0|\}}\Bigg\}\\
&=\sum_{k\in\mathbb{N}}\mathbb{E}\Bigg\{\beta\prod_{i\in\mathbb{N}\setminus\{k\}}\Bigg(1+\frac{\theta\ell(\sqrt{Q_i})}{\ell(\sqrt{Q_k})}T_i\Bigg)^{-1}\mathbf{1}_{\{Q_iT_i\geq Q_k\bigcup T_i=0\}}\\
&\qquad\times\prod_{y\in\Phi_2}\Bigg(1+\frac{\theta\mu_2\ell(y)}{\mu_1\ell(\sqrt{Q_k})}\Bigg)^{-1}\mathbf{1}_{\{|y|\geq\eta\sqrt{Q_k}\}}\Bigg\}\\
&=\sum_{k\in\mathbb{N}}\mathbb{E}\Bigg\{\beta\prod_{i\in\mathbb{N}\setminus\{k\}}\Bigg(1-\beta+\beta\Bigg(1+\frac{\theta\ell(\sqrt{Q_i})}{\ell(\sqrt{Q_k})}\Bigg)^{-1}\mathbf{1}_{\{Q_i\geq Q_k\}}\Bigg)\\
&\qquad\times\prod_{y\in\Phi_2}\Bigg(1+\frac{\theta\mu_2\ell(y)}{\mu_1\ell(\sqrt{Q_k})}\Bigg)^{-1}\mathbf{1}_{\{|y|\geq\eta\sqrt{Q_k}\}}\Bigg\}\\
&=\beta\sum_{k\in\mathbb{N}}\int_0^\infty\frac{r^{k-1}e^{-r}}{\Gamma(k)}\xi_{\mathrm{m}}^{!k}(\beta r/c)\xi_{\mathrm{p}}(\beta r/c)\mathrm{d}r,
\end{aligned}\tag{51}$$

where $\eta=(\mu_2/\mu_1)^{\delta/2}$ and

$$\xi_{\mathrm{m}}^{!k}(r)=\prod_{i\in\mathbb{N}\setminus\{k\}}\Bigg(1-\beta+\frac{\beta}{\Gamma(i)}\int_{\frac{cr}{\beta}}^\infty\frac{t^{i-1}e^{-t}}{1+\theta\big(\frac{cr}{\beta t}\big)^{\alpha/2}}\mathrm{d}t\Bigg),\tag{52}$$

$$\xi_{\mathrm{p}}(r)=\exp\left(-\pi\lambda_2\eta^2T(\alpha,\theta)r\right).\tag{53}$$

By substituting (52) and (53) into (51), we obtain (40).

When the user accesses a PBS, i.e., $\mu_2\ell(x_0)>\mu_1\ell(x)$, where $x_0\in\Phi_2$ and $x\in\Phi_1$, we have

$$P_{\mathrm{p}}(\theta)=\mathbb{P}(\mathrm{SIR}>\theta, x_0\in\Phi_2)$$

$$
\begin{aligned}
&= \mathbb{E}\left\{\exp\left(-\frac{\theta}{\mu_2\ell(x_0)}\left(\sum_{x\in\Phi_1}\mu_1\ell(x)h_x+\sum_{y\in\Phi_2^!}\mu_2\ell(y)h_y\right)\right)\mathbf{1}_{x_0\in\Phi_2}\right\}\\
&= \mathbb{E}\left\{\prod_{x\in\Phi_1}\left(1+\frac{\theta\mu_1\ell(x)}{\mu_2\ell(x_0)}\right)^{-1}\mathbf{1}_{\{|x|\geq|x_0|/\eta\}}\prod_{y\in\Phi_2^!}\left(1+\frac{\theta\ell(y)}{\ell(x_0)}\right)^{-1}\right\}\\
&= \int_0^\infty\prod_{i\in\mathbb{N}}\left(1-\beta+\beta\int_{\frac{r}{\omega\beta}}^\infty\frac{t^{i-1}e^{-t}}{\Gamma(i)\left(1+\frac{\theta r^{\alpha/2}}{(\omega\beta t)^{\alpha/2}}\right)}\mathrm{d}t\right)e^{-T(\alpha,\theta)r}\mathrm{d}r. \qquad (54)
\end{aligned}
$$

By substituting (51) and (54) into (2), we obtain the result.

References

[1] H. Wei, N. Deng, W. Zhou, and M. Haenggi, "A simple approximative approach to the SIR analysis in general heterogeneous cellular networks," in *IEEE Global Communications Conference (GLOBECOM15)*, San Diego, CA, USA, Dec. 2015.

[2] A. Ghosh, N. Mangalvedhe, R. Ratasuk, B. Mondal, M. Cudak, E. Visotsky, T. Thomas, J. Andrews, P. Xia, H. Jo, H. Dhillon, and T. Novlan, "Heterogeneous cellular networks: From theory to practice," *IEEE Commun. Mag.*, vol. 50, no. 6, pp. 54–64, Jun. 2012.

[3] H. S. Dhillon, R. K. Ganti, F. Baccelli, and J. G. Andrews, "Modeling and analysis of K-tier downlink heterogeneous cellular networks," *IEEE J. Sel. Areas Commun.*, vol. 30, no. 3, pp. 550–560, Apr. 2012.

[4] A. Guo and M. Haenggi, "Spatial stochastic models and metrics for the structure of base stations in cellular networks," *IEEE Trans. Wireless Commun.*, vol. 12, no. 11, pp. 5800–5812, Nov. 2013.

[5] N. Deng, W. Zhou, and M. Haenggi, "The Ginibre point process as a model for wireless networks with repulsion," *IEEE Trans. Wireless Commun.*, vol. 14, no. 1, pp. 107–121, Jan. 2015.

[6] M. Haenggi, "The mean interference-to-signal ratio and its key role in cellular and amorphous networks," *IEEE Wireless Commun. Lett.*, vol. 3, no. 6, pp. 597–600, Dec. 2014.

[7] G. Nigam, P. Minero, and M. Haenggi, "Coordinated multipoint joint transmission in heterogeneous networks," *IEEE Trans. Commun.*, vol. 62, no. 11, pp. 4134–4146, Nov. 2014.

[8] S. Mukherjee, "Distribution of downlink SINR in heterogeneous cellular networks," *IEEE J. Sel. Areas Commun.*, vol. 30, no. 3, pp. 575–585, Apr. 2012.

[9] N. Deng, W. Zhou, and M. Haenggi, "Heterogeneous cellular network models with dependence," *IEEE J. Sel. Areas Commun.*, vol. 33, no. 10, pp. 2167–2181, Oct. 2015.

[10] I. Nakata and N. Miyoshi, "Spatial stochastic models for analysis of heterogeneous cellular networks with repulsively deployed base stations," *Perform. Eval.*, vol. 78, pp. 7–17, Aug. 2014.

[11] V. Suryaprakash, J. Moller, and G. Fettweis, "On the modeling and analysis of heterogeneous radio access networks using a Poisson cluster process," *IEEE Trans. Wireless Commun.*, vol. 14, no. 2, pp. 1035–1047, Feb. 2015.

[12] H. Nagamatsu, N. Miyoshi, and T. Shirai, "Padé approximation for coverage probability in cellular networks," in *Proc. 12th Int. Symp. on Modeling and Optimization in Mobile, Ad Hoc, and Wireless Networks (WiOpt)*, Hammamet, Tunisia, May 2014, pp. 693–700.

[13] A. Guo and M. Haenggi, "Asymptotic deployment gain: A simple approach to characterize the SINR distribution in general cellular networks," *IEEE Trans. Commun.*, vol. 63, no. 3, pp. 962–976, Mar. 2015.

[14] R. K. Ganti and M. Haenggi, "SIR asymptotics in general cellular network models," in *Proc. IEEE Int. Symp. Inf. Theory (ISIT)*, Hong Kong, China, Jun. 2015, pp. 1009–1013.

[15] ——, "Asymptotics and approximation of the SIR distribution in general cellular networks," *IEEE Trans. Wireless Commun.*, vol. 15, no. 3, Mar. 2016. To be published.

[16] M. Haenggi, "ASAPPP: A simple approximative analysis framework for heterogeneous cellular networks," presented at Workshop on Heterogeneous and Small Cell Networks (HetSNets'14), Dec. 2014 [Online]. Available: http://www3.nd.edu/~mhaenggi/talks/hetsnets14.pdf.

[17] ——, "Mean interference in hard-core wireless networks," *IEEE Commun. Lett.*, vol. 15, no. 8, pp. 792–794, Aug. 2011.

[18] X. Zhang and M. Haenggi, "A stochastic geometry analysis of inter-cell interference coordination and intra-cell diversity," *IEEE Trans. Wireless Commun.*, vol. 13, no. 12, pp. 6655–6669, Dec. 2014.

[19] J. Andrews, F. Baccelli, and R. Ganti, "A tractable approach to coverage and rate in cellular networks," *IEEE Trans. Commun.*, vol. 59, no. 11, pp. 3122–3134, Nov. 2011.

[20] M. Haenggi, "On distances in uniformly random networks," *IEEE Trans. Inf. Theory*, vol. 51, no. 10, pp. 3584–3586, Oct. 2005.

[21] ——, *Stochastic geometry for wireless networks*. Cambridge, U.K.: Cambridge Univ. Press, 2012.

[22] S. Singh and J. Andrews, "Joint resource partitioning and offloading in heterogeneous cellular networks," *IEEE Trans. Wireless Commun.*, vol. 13, no. 2, pp. 888–901, Feb. 2014.

[23] J. Gomez, A. Vasseur, A. Vergne, P. Martins, L. Decreusefond, and W. Chen, "A case study on regularity in cellular network deployment," *IEEE Wireless Commun. Lett.*, vol. 4, no. 4, pp. 421–424, Aug. 2015.

[24] N. Miyoshi and T. Shirai, "A cellular network model with Ginibre configured base stations," *Adv. Appl. Probab.*, vol. 46, no. 3, pp. 832–845, Sep. 2014.

[25] ——, "Cellular networks with α-Ginibre configurated base stations," in *The Impact of Applications on Mathematics*. Springer, 2014, pp. 211–226.

Haichao Wei received the B.S. degree in electronic engineering from the University of Science and Technology of China (USTC), Hefei, China, in 2010. He is currently working toward the Ph.D. degree in electronic engineering at USTC. His research interests include heterogeneous and cellular networks, stochastic geometry, green communications, and underwater acoustic communications.

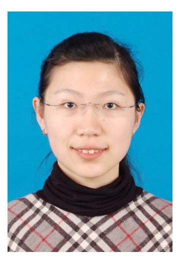

Na Deng received the B.S. and Ph.D. degrees in electronic engineering from the University of Science and Technology of China (USTC), Hefei, China, in 2010 and 2015, respectively. During her Ph.D. study, she was a Visiting Student in Prof. Martin Haenggi's Group at the University of Notre Dame, Notre Dame, IN, USA from August 2013 to August 2014. After graduation, she joined Huawei Technologies (Shanghai) Co., Ltd. Her research interests include heterogeneous and cellular networks, stochastic geometry, point process theory, green communications, and cooperative communications.

Wuyang Zhou (M'09) received the B.S. and M.S. degrees from Xidian University, Xi'an, China, in 1993 and 1996, respectively, and the Ph.D. degree from the University of Science and Technology of China, Hefei, China, in 2000. He is currently a Professor of wireless communication networks with the Department of Electronic Engineering and Information Science, University of Science and Technology of China. He participated in the National 863 Research Project Beyond Third Generation of Mobile System in China (FUTURE Plan) and has been a Task Director in many projects, including Innovative Wireless Campus Experimental Networks Research on High Frequency Networking Technologies, and Research on Transmission and Networking Technologies in Satellite Mobile Communications. His research interests include cooperative communications, radio resource management, wireless networking, satellite mobile communications, and underwater acoustic communications.

Martin Haenggi (S'95-M'99-SM'04-F'14) received the Dipl.-Ing. (M.Sc.) and Dr.sc.techn. (Ph.D.) degrees in electrical engineering from the Swiss Federal Institute of Technology in Zurich (ETH) in 1995 and 1999, respectively. After a postdoctoral year at the University of California in Berkeley, he joined the University of Notre Dame, IN, USA, in 2001, where he currently is a Professor of electrical engineering and a Concurrent Professor of applied and computational mathematics and statistics. In 2007-2008, he was a visiting professor at the University of California at San Diego, and in 2014-2015 he was an Invited Professor at EPFL, Switzerland. He is a co-author of the monograph "Interference in Large Wireless Networks" (NOW Publishers, 2009) and the author of the textbook "Stochastic Geometry for Wireless Networks" (Cambridge University Press, 2012). His scientific interests include networking and wireless communications, with an emphasis on cellular, amorphous, ad hoc, cognitive, and sensor networks. He served an Associate Editor of the Elsevier Journal of Ad Hoc Networks from 2005-2008, of the IEEE Transactions on Mobile Computing (TMC) from 2008-2011, and of the ACM Transactions on Sensor Networks from 2009-2011, and as a Guest Editor for the IEEE Journal on Selected Areas in Communications in 2008-2009 and the IEEE Transactions on Vehicular Technology in 2012-2013. He also served as a Steering Committee member of the TMC from 2011-2013, as a Distinguished Lecturer for the IEEE Circuits and Systems Society in 2005-2006, as a TPC Co-chair of the Communication Theory Symposium of the 2012 IEEE International Conference on Communications (ICC'12) and of the 2014 International Conference on Wireless Communications and Signal Processing (WCSP'14), as a General Co-chair of the 2009 International Workshop on Spatial Stochastic Models for Wireless Networks (SpaSWiN'09) and the 2012 DIMACS Workshop on Connectivity and Resilience of Large-Scale Networks, and as a Keynote Speaker of SpaSWiN'13, WCSP'14, and the 2014 IEEE Workshop on Heterogeneous and Small Cell Networks. Presently he is the Chair of the Executive Editorial Committee of the IEEE Transactions on Wireless Communications. For both his M.Sc. and Ph.D. theses, he was awarded the ETH medal, and he received a CAREER award from the U.S. National Science Foundation in 2005 and the 2010 IEEE Communications Society Best Tutorial Paper award.